Phytohormonal and Transcriptomic Response of Hulless Barley Leaf in Response to Powdery Mildew Infection

Zha Sang [1,2,†]**, Minjuan Zhang** [3,†]**, Wang Mu** [1,2]**, Haizhen Yang** [1,2]**, Chunbao Yang** [1,2] **and Qijun Xu** [1,2,*]

[1] State Key Laboratory of Hulless Barley and Yak Germplasm Resources and Genetic Improvement, Lhasa 850002, China; zhasang13518948935@taaas.org (Z.S.); wm1252354663@163.com (W.M.); 17788673107@163.com (H.Y.); yangchunbaohnb@sina.cn (C.Y.)

[2] Research Institute of Agriculture, Tibet Academy of Agricultural and Animal Husbandry Sciences Lhasa, Tibet 850002, China

[3] Wuhan Metware Biotechnology Co., Ltd., Wuhan 430070, China; zhangmingjuan8@163.com

* Correspondence: xqj18100988236@126.com or xuqijun1025@taaas.org

† Same contribution: Zha Sang, Minjuan Zhang.

Abstract: Powdery mildew (PM) caused by *Blumeria graminis* (DC.) Golovin ex Speer f. sp. hordei Marchal (*Bgh*) is one of the major yield reducing diseases in hulless barley (*Hordeum vulgare* L. var. nudum Hook. f.). Genotypes with contrasting resistance to PM offer unique opportunities to explore the transcriptome in order to understand the expression changes in genes and pathways. In this study, we explored the phytohormone levels and transcriptome of a *Bgh* susceptible (XL19) and resistant (ZYM1288) hulless barley genotypes at 0, 5, 12, 24, and 36 h post infection (hpi) with *Bgh*. We found relatively higher levels of abscisic acid, jasmonic acid, salicylic acid, and cytokinins in ZYM1288. The transcriptome analyses identified 31,354 genes that were enriched in signaling, energy, and defense related pathways. Higher numbers of differentially expressed genes (DEGs) were found in XL19 as compared to ZYM1288 after 5 (3603 vs. 2341) and 12 hpi (3530 vs. 2416). However, after 24 and 36 hpi, the number of DEGs was higher in ZYM1288 as compared to XL19 i.e., 3625 vs. 3034 and 5855 vs. 2725, respectively. Changes in hormone levels drove downstream expression changes in plant-hormone signaling that helped ZYM1288 to perform better under *Bgh* infection. The expression of DEGs in MAPK-signaling and Toll-like receptor signaling pathways, glucosinolate biosynthesis, glutathione metabolism, brassinosteroid metabolism, and energy related pathways indicated their common roles in defense against PM. Key genes related to PM-resistance were upregulated in the resistant genotype. These genes provide key information towards differences in both genotypes towards resistance to PM. The transcriptomic signatures explored in this study will broaden our understanding towards molecular regulation of resistance to PM in hulless barley.

Keywords: barley; Mlo; Mla; MAPK-signaling; photosynthesis; plant-pathogen interaction; phytohormone-signaling

1. Introduction

Hulless barley (*Hordeum vulgare* L. var. nudum Hook. f.) is an important cereal and used in human food, animal feed, and malt products. Particularly, it is an economically important crop for people living in Qingzang highland (including Tibet) [1]. It adapts well in the highlands and can withstand extreme highland conditions, therefore, it has become a principal food of Tibetans [2]. One of the major biotic stresses in barley is the powdery mildew (PM) caused by *Blumeria graminis* (DC.) Golovin ex Speer f. sp. *hordei* Marchal (*Bgh*) and it can cause yield loss up to 25% [3]. It has been reported that PM causes reduction in 1000-kernel weight, crude protein content, and yield in monocots such as winter wheat and barley [4,5].

Bgh has characteristics such as a repertoire of *Avr* genes, asexual haploid spores, and genetic recombination ability during the growing season, which support its rapid

evolution [6]. The control of PM is achieved by the exogenous application of fungicides, particularly those based on sulfur. However, such methods have their own disadvantages in terms of disturbance to climate and pose ecological risks [7,8]. Apart from this strategy, the understanding of the genetic mechanism of resistance to PM and genetically modifying the specific genes is a long-term control strategy. In Arabidopsis, the resistance is governed by *MILDEW RESISTANCE LOCUS O* (*MLO*) gene family members, *PENETRATION* proteins (*PEN1, PEN2/3*), *SYNTAXIN OF PLANTS* (*SYP*), and *CYP79B2s* [9]. Generally, the plants harbor basal resistance mechanisms such as pathogen-associated molecular patterns (PAMPs) and R-gene-mediated resistance [10]. Specific to *Bgh* in barley, a number of genes belonging to *Mla* and *Mlo* gene families have been identified [11]. The *Mla* proteins recognize fungal *Avr* genes and may require molecular chaperons (such as *RAR1* and *RAR2*) [12,13]. On the other hand, recessive mutations *Mlo* gene(s) confer durable resistance to *Bgh*, however these genes are also associated with pleotropic effects and exhibit spontaneous necrosis leading to loss of photosynthetic area and yield [14]. This knowledge has been used to develop multiple resistant genotypes (containing *mlo* broad spectrum resistance) in different parts of world (e.g., Europe and Ethiopia) [14,15]. Other modulators of the innate immune response in plants such as *CYP79B2*, *CYP79B3*, *WRKY21*, suppressor of the G2 allele of skp1 (*SGT1*), S-phase kinase-associated protein 1 (*SKP1*), molecular chaperones (*HSP90*), *RPM* genes, and other resistance related genes i.e., disease resistance gene analogs (RGAs) have also been implicated in defense responses against PM [15–17].

Breeding efforts are being extended to explore further genes and pathways that can significantly contribute to increased resistance to PM (broad-specific resistance). In this regard, developments in genomics are aiding the discovery and detailed understanding of the resistance strategies in crop plants against PM. For example, a recent study compared the transcriptome of contrasting barley varieties and reported that mitogen-activated protein kinase (MAPK) and other signaling mechanisms i.e., plant-hormone signaling pathway are activated in response to *Bgh* [18]. In wheat, cell-wall fortification, flavonoid biosynthesis, and metabolic process have been reported to play roles in resistant genotypes [18]. In grapevine, PM induces defense-related transcriptional reprogramming and the levels of defense related hormones (salicylic acid, SA) increase [19]. In melon (*Cucumis melo* L.) phytoalexin biosynthesis and primary metabolite related transcriptome were highly regulated when infected with PM [20]. A recent study on barley near isogenic lines carrying various resistance genes reported that PM induces changes in phytohormones as well as photosynthesis [21]. These recent studies opened new avenues for exploring the possible mechanisms that can enhance broad spectrum resistance against PM. In order to further understand the PM resistance mechanisms and strategies, large scale transcriptomic studies can be a promising approach. This will lead towards a better understanding of the transcriptomic signatures that might be involved in the regulation of changes in phytohormones, energy related process, and particularly the signaling mechanisms/pathways in PM resistant hulless barley.

In an ongoing experiment focused on the screening of Chinese hulless barley varieties, we identified two genotypes that showed contrasting resistance/susceptibility patterns against PM i.e., XL19 showed susceptibility to *Bgh*, while ZYM1288 was resistant. The present study was designed to explore the differences in foliar transcriptome and phytohormone levels of both genotypes. We employed LC-MS/MS and Illumina HiSeq RNA-sequencing to identify the key hormone changes and differential regulation of signaling, energy, and defense related pathways at 0, 5, 12, 24, and 36 h post infection (hpi).

2. Results

2.1. Phytohormonal Response of XL19 and ZYM1288

The PM inoculation resulted in visible increased leaf yellowing symptoms in the susceptible genotype XL19, while the resistant genotype ZYM1288 showed relatively fewer leaf yellowing signs (Figure 1). This yellowing is indicative of the fact that the disease is established, and the fungus is depleting the leaf of nutrients. It is known that the

establishment of PM induces changes in phytohormones [21]. The phytohormone analysis showed that at 5 hpi, the abscisic acid (ABA) level increased in XL19 and decreased in ZYM1288 as compared to their respective controls. At this time point, XL19 showed higher ABA levels than ZYM1288. At 12, 24, and 36 hpi the ABA levels in XL19 and ZYM1288 were reduced as compared to 0 hpi, where the latter had higher levels as compared to the XL19. (Figure 2i). The auxin levels varied between different time points and showed no trend for indole 3-acetic acid (IAA); the IAA levels increased at 5, and 12 hpi in XL19 and then remained more or less constant at 24 and 36 hpi as compared to 0 hpi. ZYM1288 showed reduced IAA contents in all time points except 24 hpi, where the IAA levels were slightly increased (Figure 2ii). The methylindole-3-acetic acid (ME-IAA) levels in ZYM1288 were lower in all the time points as compared to 0 hpi, while in case of XL19, the ME-IAA levels did not show any trend (Figure 2iii). The indole-3-carboxylic acid (ICA) levels in ZYM1288 were lower than the controls. However, it is to be noted that after 12 and 36 h, then ICA levels were reduced to less than half as compared to the control. In XL19, the ICA contents increased after 5 and 12 hpi, while remained more or less same after 24 and 36 hpi (Figure 2iv). Among all auxins, the Indole-3-carboxaldehyde (ICA-Id) levels showed a decreasing trend in both genotypes with XL19 showed minor reductions while ZYM1288 showed observable reductions and decreased with time ongoing except at 36 hpi (Figure 2v). The level of dihydrojasmonic acid (H2JA) dropped after the PM infection at all time points, where the susceptible genotype had relatively lower levels when compared with the ZYM1288 (Figure 2vi). The jasmonic acid (JA) levels were lower in ZYM1288 and XL19 after PM infection as compared to their respective controls. However, interestingly, the levels were higher after 12 hpi in XL19. Similar levels of JA were recorded in ZYM1288 after 12 hpi though still lower than 0 hpi (Figure 2vii). Jasmonoyl-L-Isoleucine (JA-ILE) level decreased in ZYM1288. Overall, JA-ILE levels were lower in XL19 except for 12 hpi (Figure 2viii). The methyl Jasmonate (MEJA) levels in XL19 remained more or less constant but in the resistant genotype, the level increased with time until 24 hpi as compared to 0 hpi (Figure 2ix). Salicylic acid (SA) differed between the genotypes. It was slightly reduced at 5 and 12 hpi then increased at 24 hpi but again reduced at 36 hpi in ZYM1288. In case of XL19, the SA levels were lower after 5, 12, and 24 hpi, while higher after 36 hpi (Figure 2x). It is to be noted that ZYM1288 had higher tZ levels as compared to its control, while in case of XL19, a significant rise was observed at 5 hpi and then the levels decreased unit 24 hpi (but still higher than 0 hpi) and after 36 hpi, the levels were lower than 0 hpi. ZYM1288 had higher trans-zeatin (tZ) levels than XL19 except at 5 hpi (Figure 2xi).
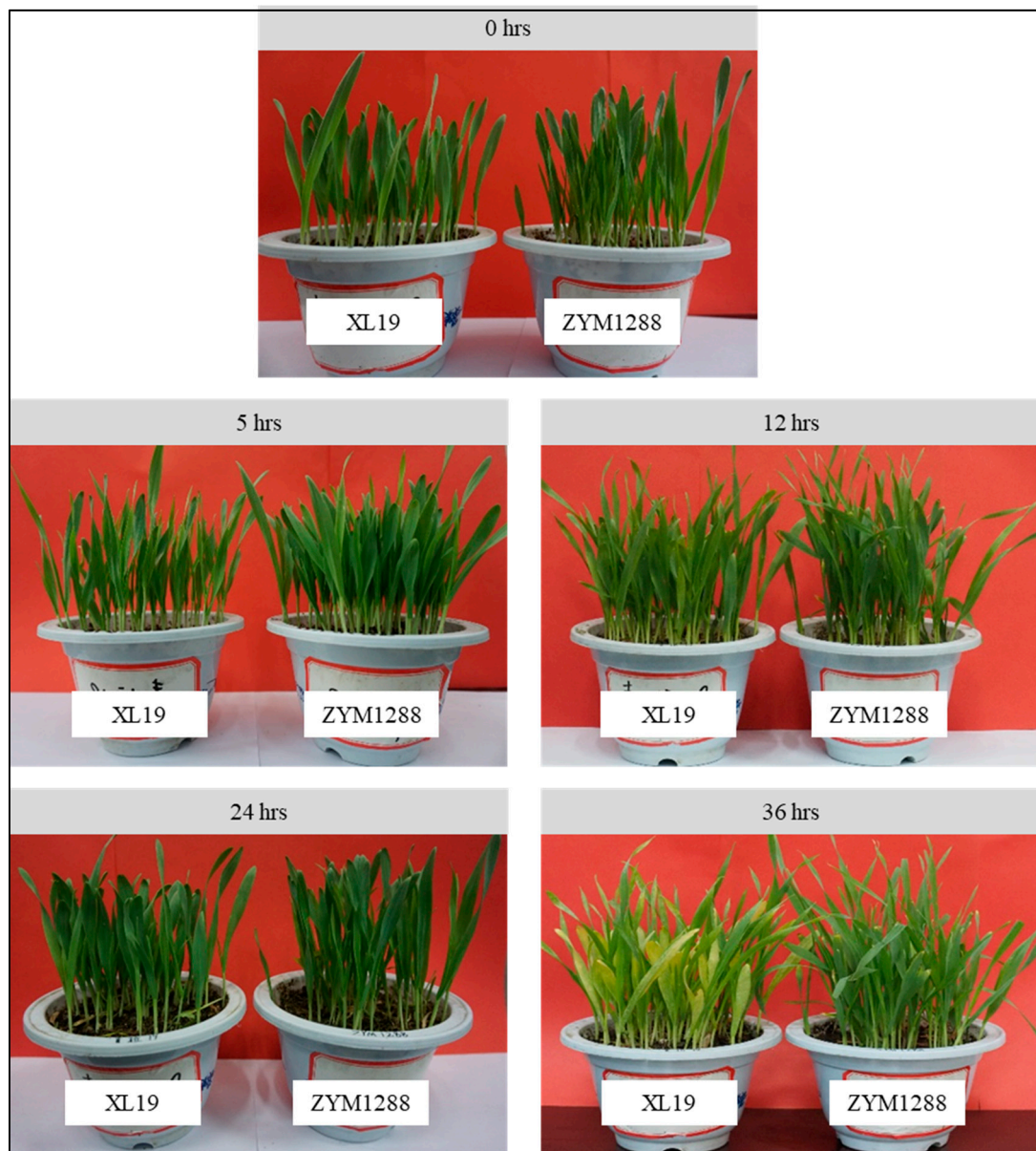
Figure 1. XL19 and ZYM1288 hulless barley genotypes infected with *Bgh* after 0 (CK), 5, 12, 24, and 36 h.
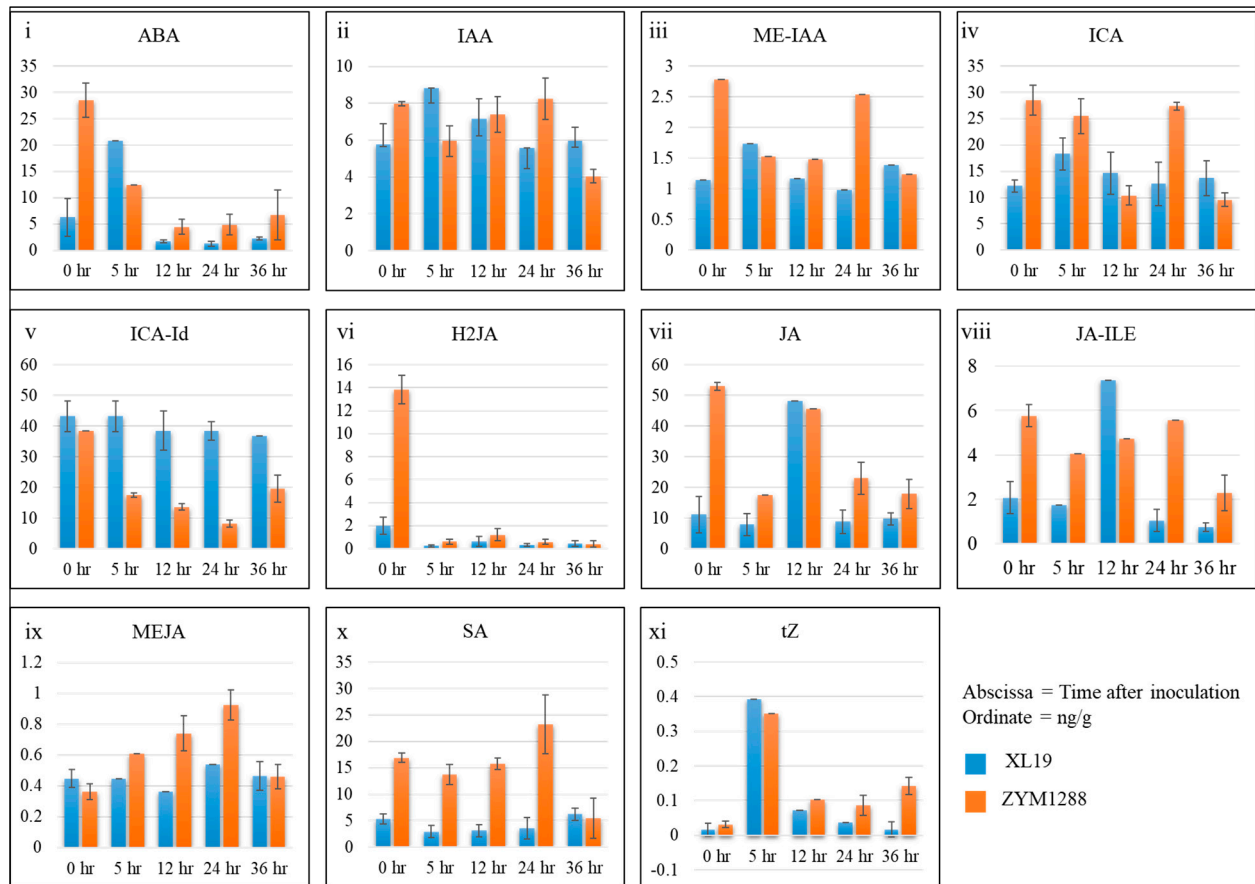
Figure 2. Phytohormonal concentrations in XL19 and ZYM1288 after 0 (CK), 5, 12, 24, and 36 hpi; (**i**) abscisic acid (ABA), (**ii**) indole 3-acetic acid (IAA), (**iii**) methylindole-3-acetic acid (ME-IAA), (**iv**) indole-3-carboxylic acid (ICA), (**v**) Indole-3-carboxaldehyde (ICAId), (**vi**) dihydrojasmonic acid (H2JA), (**vii**) Jasmonic acid (JA), (**viii**) (±)-Jasmonic acid-isoleucine (JA-ILE), (**ix**) methyl Jasmonate (MEJA), (**x**) Salicylic acid (SA), and (**xi**) trans-zeatin (tZ). The error bars represent standard deviation.

2.2. Transcriptomic Responses of XL19 and ZYM1288

The transcriptome of 30 leaf samples (2 genotypes × 5 time points × 3 biological replicates) resulted in 46.25–67.55 million clean reads (average 56.35 million clean reads and 253.59 Gb clean data). The Q30% was ≥93.2% and the average GC content was 56.56%. The clean reads were then mapped to the reference genome [22] and 31,354 genes were obtained (Supplementary Table S1).

The Fragments Per Kilobase of Transcript per Million fragments mapped (FPKM) for XL19 was higher in infected samples as compared to CK. Similarly, the FPKM values in infected ZYM1288 leaves were higher except for 36 hpi. The average Pearson Correlation Coefficient (PCC) for the biological replicates was ~0.79 (Figure 3a) indicating the reproducibility of the experiment and the reliability of expression data. Higher number of differentially expressed genes (DEGs) was found in XL19 as compared to ZYM1288 after 5 (3603 vs. 2341) and 12 hpi (3530 vs. 2416). However, after 24 and 36 hpi, the number of DEGs was higher in ZYM1288 as compared to XL19 i.e., 3625 vs. 3034 and 5855 vs. 2725, respectively (Figure 3b). We found 1076 DEGs that were common between all treatment comparisons in both genotypes (Figure 3c). The KEGG pathway enrichment showed that the DEGs were enriched in a large number of pathways related to signaling (plant hormone signaling, MAPK signaling, Toll-like receptor signaling, and plant-pathogen signaling) and energy related pathways (photosynthesis, photosynthesis-antenna proteins, galactose metabolism, starch and sucrose metabolism, nitrogen metabolism, pentose phosphate pathway, citrate cycle, and carbon fixation in photosynthetic organisms). Further, the DEGs

were enriched in several defense related pathways such as secondary metabolite biosynthesis, brassinosteroid metabolism, glutathione metabolism, and glucosinolates biosynthesis (Supplementary Figure S1; Supplementary Table S2).
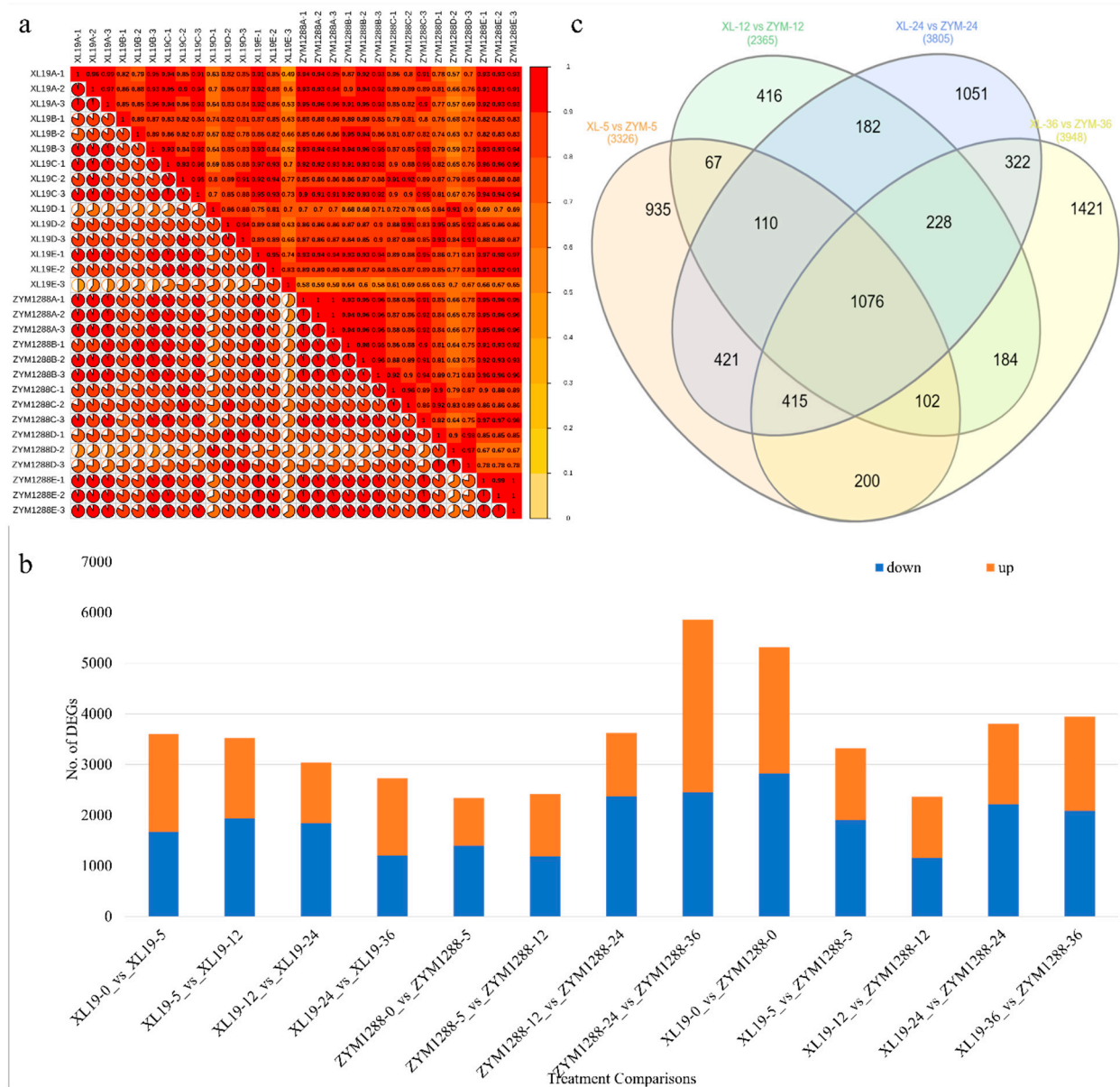

Figure 3. (**a**) Pearson correlation coefficient between the expression of biological replicates, (**b**) number of differentially expressed genes between different treatment comparisons, and (**c**) venn diagram of differentially expressed genes at different time points in susceptible (XL19) and resistant (ZYM1288) hulless barley. A, B, C, D, and E in figure panel a represent 0, 5, 12, 24, and 36 hpi, respectively.

2.3. Differential Gene Expression between XL19 and XYM1288

2.3.1. Signaling Responses

a. Plant hormone signal transduction.

Powdery mildew infection in other plants such as pumpkin had shown the differential regulation of plant-hormone signaling pathway, which is consistent with our results [23]. Highest number of DEGs were enriched in auxin signaling part of this pathway (Figure 4). The auxin induced proteins (AUXs) were downregulated in ZYM1288 while the auxin transporter protein 1 was upregulated. Additionally, the *ARF*s or *ARF/IAA*s showed differ-

ent regulation patterns, particularly *ARF/IAA21*, *ARF18*, three *ARF19*s, *ARF5* and *ARF7*s were upregulated after 36 h in ZYM1288, while these genes did not differentially express at other time points. One *ARF/IAA30* was upregulated throughout the four time points in the resistant genotype. Contrastingly, the *ARF2* and *ARF11*s were downregulated in at least one time point in ZYM1288. The *GH3.8*, and *SUAR*s' expression increased in ZYM1288 after infection as compared to XL19, indicating that XL19 is unable to continue cell enlargement and plant growth (Figure 4). Contrary to auxins, only six cytokinin signaling related genes i.e., histidine kinases (HKs; *HK3*, *HK4*) pseudo histidine-containing phosphotransfer protein 5 (*PHP5*), two-component response regulations (*ORR*s; *ORR1*, *ORR3*, and *ORR26*) were differentially expressed. The upregulation of these genes (except *HK3*) is indicative of higher cytokinin signaling in ZYM1288, which is consistent with tZ levels (Figures 2xi and 4). We found that 14 of 15 DEGs enriched in ABA signaling pathway were upregulated in ZYM1288 as compared to XL19 in at least one time point, which is in agreement with ABA levels (Figure 2). Together with the higher ABA levels in ZYM1288 leaves, the upregulation of key DEGs benefits the resistant genotype and enhances its resistance against PM, which is consistent with a recent report on barley near-isogenic lines [21]. Similar to this, all the DEGs enriched in gibberellin signaling were upregulated in ZYM1288 except *TIF1-like* gene. An important observation was that the log2 FC values of these DEGs in XL19/ZYM1288 were higher in all time points. These expression changes indicate that ZYM1288 shows resistance to PM by increased degradation of DELLAs as indicated by increased upregulation of *GID2* and *GAI*s (Figure 4) [24]. Additionally, the DEGs were enriched in ethylene, brassinosteroid, JA, and SA signaling. It is known that SA, JA, and ethylene enhances defense against pathogens. Thus, the increased accumulation and upregulation of related genes enhances the resistance of ZYM1288 against PM (Figure 4).

b. MAPK signaling pathway and Toll-like receptor signaling pathway.

A previous study on Arabidopsis has shown the involvement of MAPK signaling pathway against PM infection [25]. The KEGG pathway enrichment analysis also indicated that 101 DEGs were enriched in this pathway. Major genes i.e., *ANP1*, *CALM*, *CAT*, *CHI-B*, *EBF1*, *EIN3*, *ERECTA*, *ERF*s, *FLS*2s, *MAPK*s, *MAP2K*s, *MAP3K*s, *MYC2*, *PRP*s, *PP2C*s, *PYR/PYL*s, *WRKY22*s, and *WRKY33*s were differentially expressed between both genotypes at four time points as compared to CK. Most importantly, we noticed that genes involved in early and late response for pathogens i.e., *FLS2*, *MAP2K*s, and *PR2C6* were upregulated in ZYM1288 as compared to XL19 (Figure 5). The PM infection caused the upregulation of genes that are present in pathogen attack signaling and generation of H_2O_2 related part of MAPK signaling pathway. Defense against PM in ZYM1288 is possibly due to the upregulation of genes such as serine/threonine receptor kinases (*ERECTA*s), *NDPK2*, *ANP1*, and *PR2C6* (and *PRP*s). The genes related to defense response and wounding responses (a part of ethylene and JA signaling of MAPK signaling pathway) i.e., *ERF1*, *ChiB*, *MYC2*, and *VIP2* were also upregulated in ZYM1288 as compared to XL19. Taken together, it is clear from the differences in the expression in the XL19 and ZYM1288 that MAPK signaling pathway plays significant role in PM resistance or susceptibility (Figure 5).

Another important signaling pathway i.e., Toll-like receptor signaling pathway was one of the significantly enriched pathways between XL19 and ZYM1288 hulless barley leaves infected with PM (Supplementary Figure S1). A total of 455 DEGs were enriched in Toll-like receptor signaling pathway. Interestingly, only 9 of 455 genes were annotated as other than interleukin-1 receptor-associated kinases (*IRAK1* and *IRAK4*). Ninety *IRAK*s were upregulated in ZYM1288 at 5 hpi and at least in one of other time points i.e., 12, 24, and 36 hpi. On the contrary, relatively higher number i.e., 101 IRAKs were downregulated at 5 hpi in ZYM1288. Furthermore, the expression of toll-interacting protein, ubiquitin-conjugating enzymes (*E2-D*, and *E2-N*), *ankyrin*, and *cathepsin K* were upregulated in ZYM1288 at least in one time point. These genes are possibly affecting the increased immunity in ZYM1288 and could be candidates for gene specific characterization studies (Supplementary Table S3).
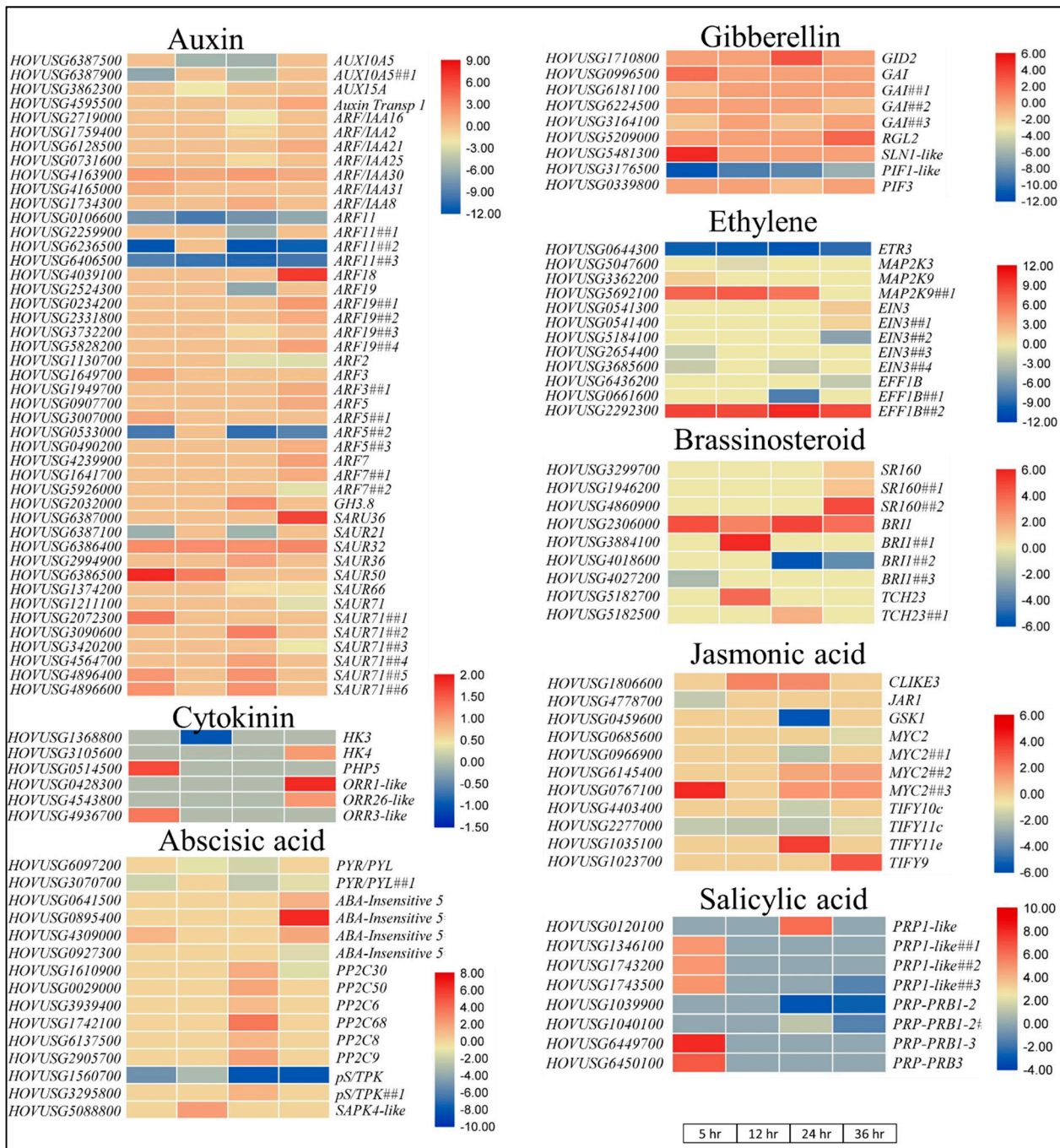
Figure 4. Heatmaps of log2 FC values of DEGs (in XL19/ZYM1288) that were significantly enriched in plant hormone signaling pathway.
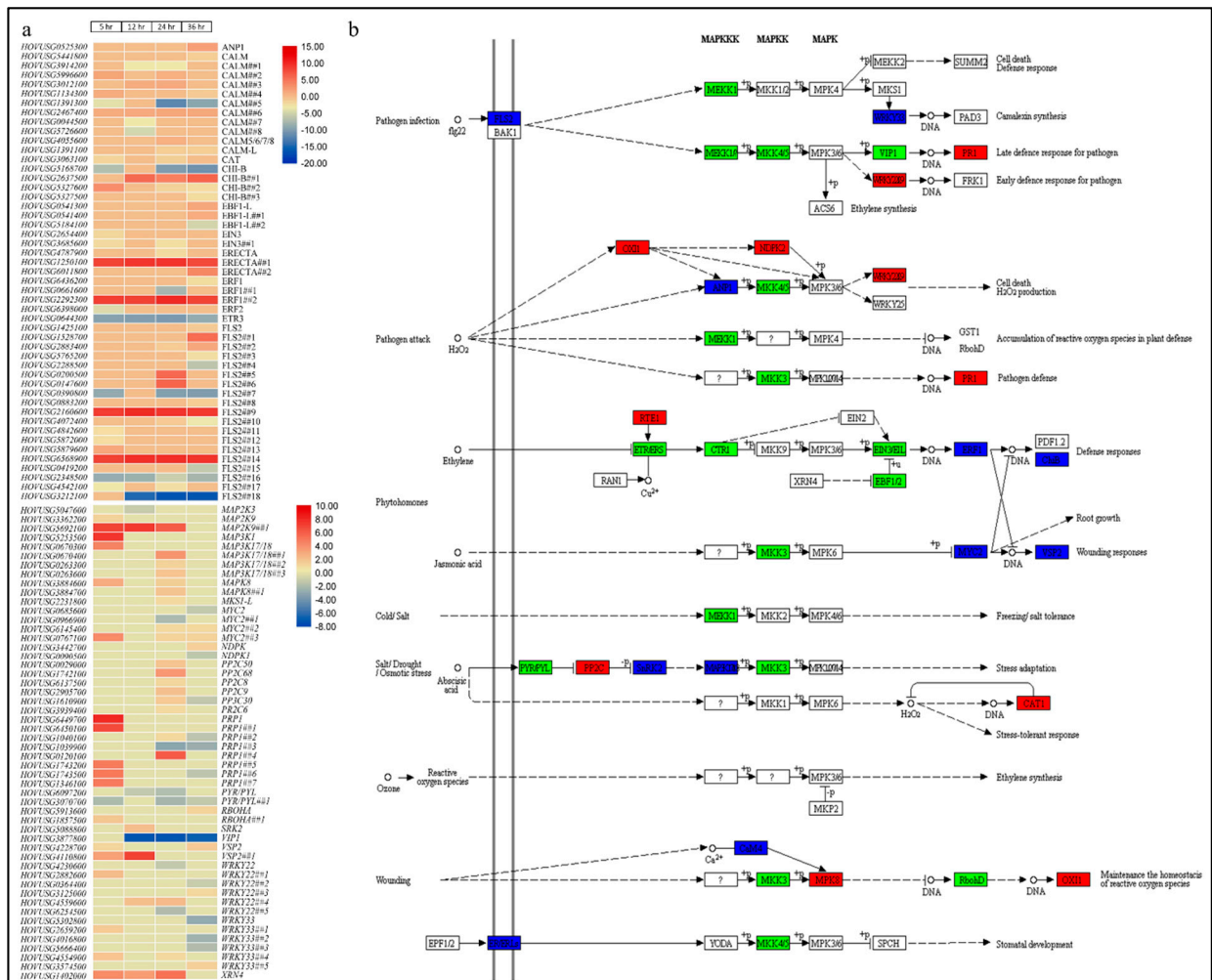
Figure 5. Regulation of MAPK signaling pathway in hulless barley in response to PM infection after 5, 12, 24, and 36 hpi. (**a**) Heatmaps showing log2 FC values of DEGs at different time points (XL19/ZYM1288). (**b**) Pathway map showing the differential regulation of MAPK signaling pathway between XL19 and ZYM1288 after 5 hpi. The genes highlighted in green, red, and blue colors represent down-, up-, and up/down-regulated DEGs.

c. Plant pathogen interaction pathway

One of the key responses in plants to pathogen attack is the activation of plant pathogen interaction pathway. It is a basic resistance pathway but includes the most important transcriptional reprogramming events that help plants to defend themselves against invading pathogens such as PM [26,27]. Between the PM infected XL19 and ZYM1288 hulless barley leaves, 233 DEGs were enriched in this pathway (Supplementary Table S5). Two CDPK genes, which cause the hypersensitive response (HR), (*HOVUSG1976600* and *HOVUSG1976900*) were upregulated in ZYM1288. Similarly, the upregulation of *CML*s and *CNGC* indicates that ZYM1288 senses changes in Ca^{2+} concentrations and responds by the stomatal closure, cell wall reinforcement, and HR. Additionally, the upregulation of many *FLS2s*, *MAP3Ks*, *HSP90kDas*, *PRPs,* and *PBS1* indicates that signaling related to the activation of defense related proteins in ZYM1288 is stronger than in XL19. The differential but not consistent regulation of effector triggered immunity (ETI) related genes such as *RINs*, *RPSs*, and a large number of *RPMs* indicate that ETI is involved in defense against PM in both genotypes. Based on the above-mentioned transcriptomic changes, it could be stated that ZYM1288 uses PAMP-triggered immunity (PTI) and ETI related genes to defend itself against the invading PM but both types of immunity mechanisms are active in the tested two genotypes.

2.3.2. Transcriptional Changes in Energy Related Pathways

Among energy related pathways, the stress effects start from the changes in photosynthetic efficiency in response to modifications in photosynthesis-antenna proteins and photosynthesis pathway [28]. Changes in these pathways are accompanied by other energy and metabolism related pathways including galactose metabolism, starch and sucrose metabolism, nitrogen metabolism, pentose phosphate pathway, citrate cycle, and carbon fixation in photosynthetic organisms [29]. The genes expressed between XL19 and ZYM1288 after the infection of PM were enriched in all the above-mentioned pathways signifying large scale transcriptional changes in energy related pathways. Eight photosystem II (PSII) proteins (*PsbW*, *P680 reaction center D1* and *D2* proteins, *CP43*, *oxygen-evolving enhancer 1* and *3*, *10 kDa protein*, and *P700 chla*), and four *ferredoxin* proteins (two *ferredoxins* and two *ferredoxin-NADP+reductases*) were differentially regulated. Only two proteins (*PsbW* and *P680 D1*) were downregulated in ZYM1288 at 5 hpi indicating that XL19 has reduced photosynthetic activity as compared to ZYM1288. Seven light-harvesting complex proteins (one *LhcI* and six *LhcII* proteins) were also differentially expressed. The *LhcI* protein (*chla/b3*) and one *LhcII* (*chla/b1*) were upregulated in ZYM1288 (Supplementary Table S4). Twenty-seven DEGs were enriched in carbon fixation in photosynthetic organisms pathway (11 up- and 16 downregulated in at least one time point in ZYM1288). One MDH (malate dehydrogenase), one phosphoenolpyruvate carboxylase (PEP), two fructose-bisphosphate aldolases (ALDOA, class I and class II), and one aspartate aminotransferase (AST) were highly downregulated in ZYM1288 as compared to XL19. However, other MDHs were upregulated at all hpi of infection in ZYM1288, suggesting that alternative (or different) key steps are being transcriptionally regulated in response to PM infection in both genotypes. Thirty-three genes were differentially expressed between both genotypes after infection; 17 were downregulated and 16 were upregulated. A higher number of DEGs (108) were enriched in starch and sucrose metabolism. The DEGs that were enriched in the above-mentioned energy related pathways showed different transcription signatures i.e., different genes with similar annotation showed contrasting expression patterns, indicating that complex transcriptomic changes are triggered in response to PM infection and both genotypes vary on how and which step of the pathway is being regulated. For example, 10 beta-fructofuranosidases were differentially regulated at different time points; five were upregulated in ZYM1288 and five were downregulated. Similarly, one MDH was highly downregulated in all time points while other MDHs were up/downregulated in at least one time point in citrate cycle. Nine nitrogen metabolism-related DEGs were found of which only three were upregulated (one *carbonic anhydrase*, one *glutamine synthase*, and a *MFS transporter*) in ZYM1288. The other DEGs in this pathway were upregulated in XL19. These expression changes further support our above statements and suggest that changes in energy metabolism related pathways discussed above are common to both genotypes, thus it could be a general response in hulless barley against PM infection (Supplementary Table S4).

2.3.3. Transcriptional Changes in Defense Related Pathways

In addition to the plant-pathogen interaction pathway, our analyses indicated the enrichment of other defense related pathways including secondary metabolite biosynthesis, brassinosteroid biosynthesis, glutathione metabolism, and glucosinolate biosynthesis (Figure 6a). Fourteen DEGs related to brassinosteroids biosynthesis were differentially regulated between both genotypes after PM infection. With prolonging infection time, the number of DEGs increased. The *steroid 22-alpha-hydroxylase* (*T9L24.4*), two *BR6-COX*, two *CYP724B1*s, a *BAS1*, and one *CYP92A6* gene were downregulated in at least one time point except 5 hpi. On the contrary, five *CYP724B1*s and two *CYP92A6*s were upregulated in ZYM1288 as compared to XL19. Both *CYP724B1* and *CYP92A6* are key players in the biosynthesis of brassinosteroids (Figure 6b) [30,31]. The upregulation of these genes suggests higher BR biosynthesis in ZYM1288 thus enhancing resistance against PM [32]. Fifty-nine genes related to glutathione metabolism were expressed between XL19 and ZYM1288 at

least at one time point after the PM infection (Figure 6c); 38 *glutathione s-transferases* (*GST*s), six *L-ascorbate peroxidases* (*APX*s), three *leucyl aminopeptidases* (*LAP*s), four *ribonucleoside-diphosphate reductase subunit M1* (*RRM1*s), two *gamma-glutamylcyclotransferase-plant* (*GGCT*s), a *glutathione synthase* (*GSS*), an *isocitrate dehydrogenase* (*IDH*), a *6-phosphogluconate dehydrogenase* (*6PGD*), and a *glutathione reductase* (*GR*). *IDH*, *LAP*s, *RRM1*s, and *GSS* were downregulated in the resistant genotype however the other genes were upregulated. In particular, we observed that a higher number of *GST*s were upregulated in different time points after infection in ZYM1288. Other than the glutathione metabolism, four DEGs (*phenylalanine N-monooxygenases, CYP79A2*) were enriched in glucosinolate biosynthesis. Three DEGs were highly downregulated in ZYM1288 as compared to XL19 and one was upregulated in all four time points, indicating important role but variable expression pattern. This gene controls the initial steps of conversion of L-phenylalanine to benzyl-glucosinolate, which is known for its vital role in systematic defense against invading pathogens [33]. The upregulation of *CYP79A2* in both genotypes indicates that it is a common defense response against PM in hulless barely. Finally, 590 genes enriched in secondary metabolite biosynthesis were differentially expressed between both genotypes after PM infection (Supplementary Table S4). The expression pattern was similar to that of energy related pathways i.e., genes with same annotation were both up- and downregulated in both genotypes indicating a significant role of secondary metabolites in defense against PM in hulless barley (Figure 6).

2.3.4. Transcriptional Changes in Known PM Related Genes

We also searched the transcriptome of PM infected XL19 and ZYM1288 hulless barley genotypes. Particularly, we searched for DEGs such as *Mlo, PEN1, SYP, SNARE, CYP79B2, CYP79B3, WRKY21, SGT1, SKP1*, and *HSP90, RPM* genes, and other resistance related genes i.e., *RGAs* based on previous reports [15–17]. We found that a *1-acyl-sn-glycerol-3-phosphate acyltransferase* (*PLSC*) was highly upregulated in ZYM1288 at all time points, while two ATP-binding cassette genes (subfamily G member 2) were downregulated at 5 hpi in ZYM1288 as compared to XL19. As discussed above, the *RPM1*s, *IRAK1*s and *IRAK4*s showed a variable expression pattern in both genotypes, while *HSP90* genes were upregulated in ZYM1288 (Figure 5; Supplementary Table S3). Similar expression pattern was observed for *RPP*s, *SYP*, and *STIP1*s (stress-induced phosphoprotein 1). Interestingly, we found a *DOWNY MILDEW 2-like* gene that was downregulated in ZYM1288 as compared to XL19 at 5, 24, and 36 hpi. Three inversins (ankyrin repeat and SOCS box protein 11-like) were upregulated in ZYM1288 as compared to XL19. The *inorganic pyrophosphatases* (*iPPase*), *multidrug resistance proteins* (*MRPs*) showed variable expression pattern in both genotypes. The known resistance genes i.e., *Mla*s were all upregulated in ZYM1288 as compared to XL19; five upregulated at 5, 12, and 24 hpi, and two upregulated all time points. Three *Mlo* proteins (*HOVUSG2614500, HOVUSG2614900* and *HOVUSG5080300*) were upregulated in XL19 at all time points after infection. These observations suggest that *Mla* genes enable ZYM1288 to resist the PM while the XL19 genotype is susceptible due to the increased expression of *Mlo* genes. A *PP2A* (serine/threonine-protein phosphatase 2A activator), a *PRMC* (*release factor glutamine methyltransferase*), a *RRM2* (*cold-inducible RNA-binding protein*). A *gamma-tubulin complex component 6* (*TUBGCP6*) were also upregulated in ZYM1288 (Figure 7).

2.3.5. qRT-PCR Analysis

The qRT-PCR analysis of seven DEGs in *Bgh* infected XL19 and ZYM1288 hulless barley genotypes was carried out using *Actin* gene as an internal control (Figure 8). The relative expression of these seven genes was consistent with that of the FPKM values. These results confirmed that the RNA-seq results are reliable.
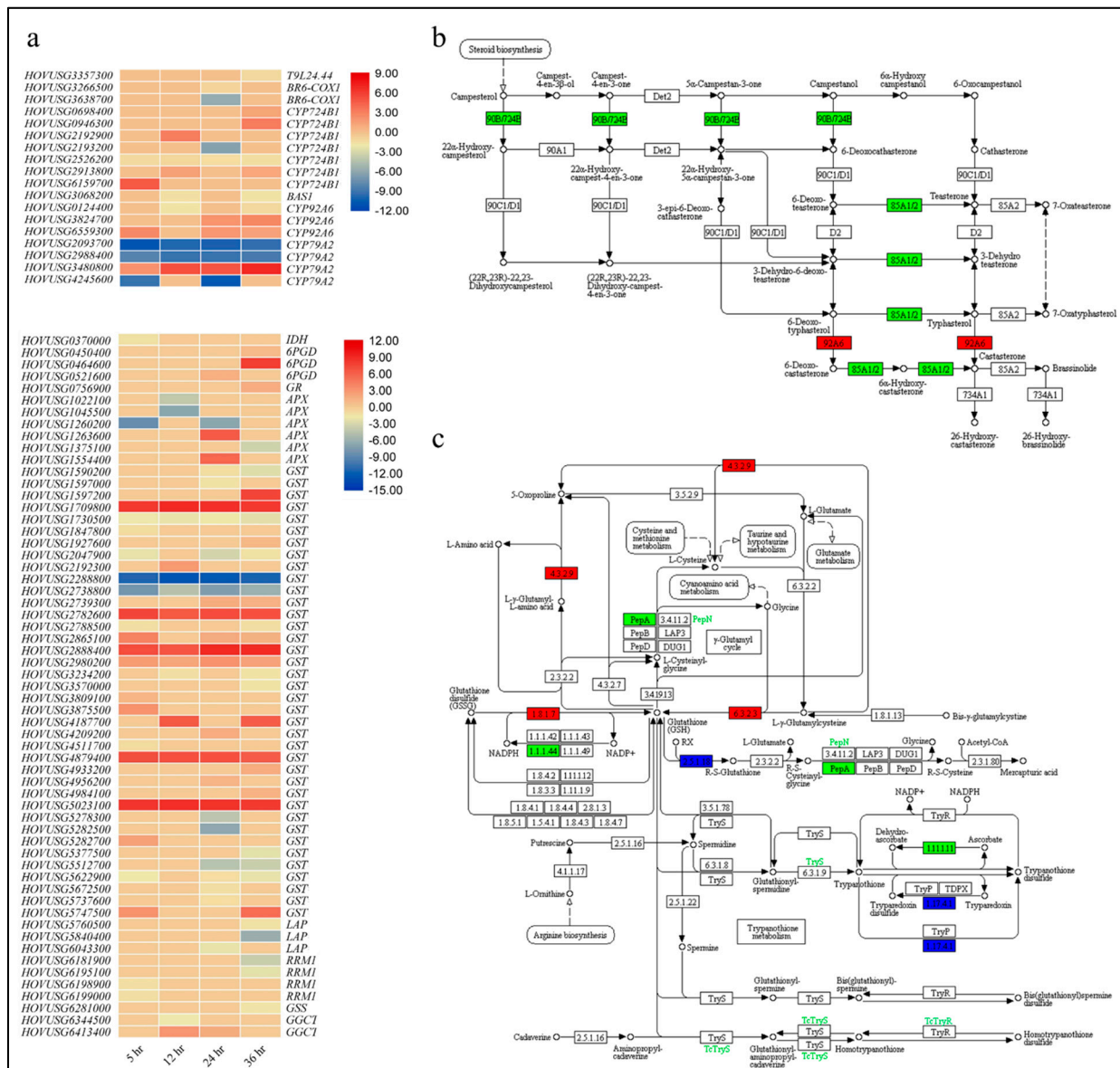
Figure 6. (**a**) Heatmap of log2 FC values of genes related to glutathione metabolism, glucosinolate biosynthesis, and brassinosteroid biosynthesis pathways that were differentially expressed in PM infected hulless barley genotypes (XL19 and ZYM1288). (**b**) Differential regulation of brassinosteroid biosynthesis pathway and (**c**) glutathione metabolism pathway between XL19 and ZYM1288 after 24 h of the PM infection. The genes highlighted in green, red, and blue colors represent down-, up-, and up/down-regulated DEGs.
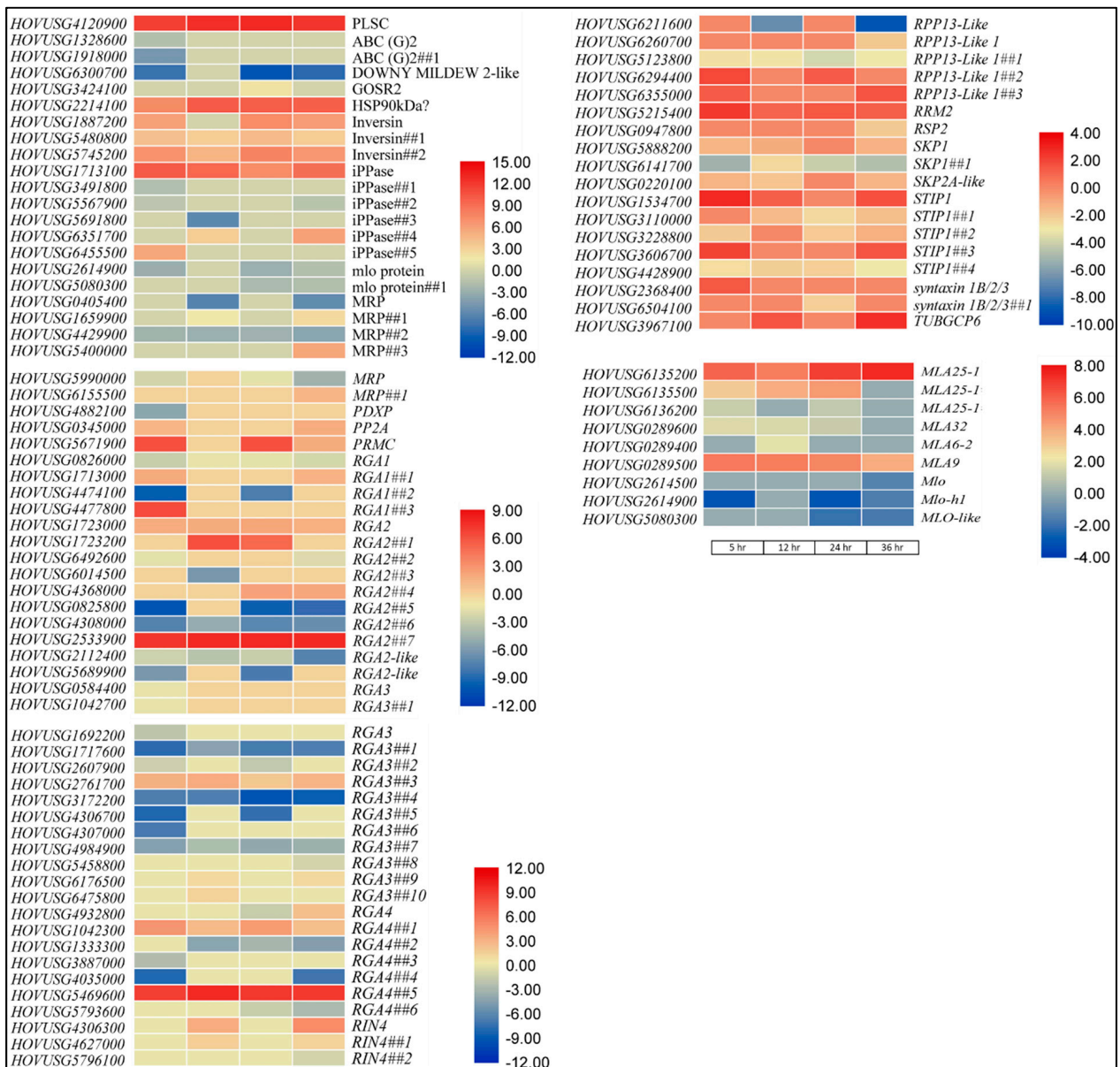
Figure 7. Heatmaps of log2 FC values of DEGs related to PM resistance that were regulated between XL19 and ZYM1288 hulless barley genotypes at 5, 12, 24, and 36 h after infection with PM.
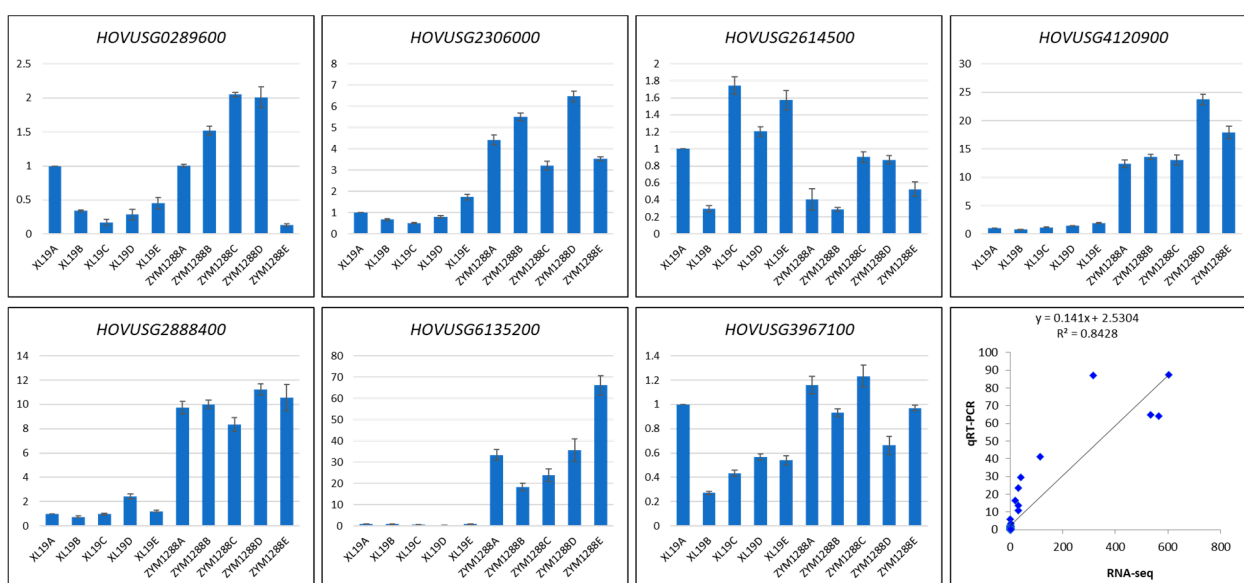
Figure 8. Quantitative real-time PCR analysis and correlation between qRT-PCR expression data and RNA-Seq data of selected DEGs in XL19 and ZYM1288. A, B, C, D, and E represent CK, and 5, 12, 24, and 36 h after the infection of *Bgh*.

3. Discussion

3.1. Phytohormone Level and Signaling Is Differentially Affected in XL19 and ZYM1288

Auxin is primarily a development related hormone, however, it also plays roles in stress responses in plants. The overlapping expression of auxin responsive genes has been particularly observed in biotic stress responses [34]. The variable levels of auxins and expression patterns of DEGs implicated in auxin signaling propose that auxins are possibly playing role in defense against PM in both genotypes used in this study. The higher expression levels of *auxin transporter 1*, *GH3.8*, and *SAUR*'s is possibly one of the main reasons that ZYM1288 leaves stayed green since these proteins influence the cell enlargement and plant growth [35]. In addition to auxin, the increased resistance of ZYM1288 might be due to higher tZ levels. We state this because of the recent reports that cytokinins can play a role as a priming agent and promote pathogen resistance and induce immunity in hosts e.g., barley [21,36]. Increased cytokinin signaling as a result of the upregulation of *HK*s, *PHP5*, and *ORR*s probably played a role in the strong defense response against PM in ZYM1288. Previously, *HK5* and *PHP*s in Arabidopsis have been shown to enhance resistance against fungal pathogens [37,38], while, *ORR*s mediate interactions between cytokinin and SA in plant immunity [39]. The strong changes in the stress hormones i.e., JA, SA, and ABA are consistent with earlier studies of barley plants (and generally in PM resistant plant species) that showed higher levels of these hormones when infected with PM [21,40]. The increased ABA levels might have triggered the high expression of signaling pathways related DEGs such as ABA-insensitive 5 (*ABI5*) (Figure 3) that induces the expression of many ABA-responsive genes involved in resistance mechanisms [41]. The increased expression of DEGs related to JA signaling i.e., *TIFYs*, *MYC2s*, *JAR1*, and *CLIKE3* and the concertation changes clearly indicates the possibility that ZYM1288 performs better and exhibits resistance to PM, probably due to increased expression of JA signaling related genes and higher JA levels, while XL19 might not. These changes are consistent with the known role of JA signaling in plant resistance to biotrophic pathogens [42]. Finally, the resistance in ZYM1288 might also be due to higher SA levels (Figure 1) and subsequent activation of many *PRP* proteins (Figure 3) [43]. Previous studies have also explored such a role of SA against PM in grapevine infected with PM [27]. Taken together, ZYM1288 shows resistance to PM possibly due to increased levels of defense related phytohormones and cytokinin and subsequent expression changes in the related signaling genes.

3.2. MAPK Signaling Pathway and Toll-Like Receptor Signaling Pathways Are Activated in Response to PM in Hulless Barley

MAPKs are evolutionarily conserved proteins in plants and are required for the activation of plant immunity [44]. MAPK signaling is one of the earliest signaling events after the plant has sensed the pathogen attack. The regulation of more than a hundred DEGs in this pathway strongly indicates the possibility that PM attack is sensed and signals are sent to downstream pathways for the activation or inactivation of genes/proteins [45] (Figure 4). Upon infection with PM, the differential expression of *FLS2*s in both genotypes suggests that *FLS2*-mediated defense response might be active; relatively higher *FLS2*s in ZYM1288 are possibly enabling its better resistance to PM [46]. We propose this since a similar expression trend of *WRKY33*s was noted in ZYM1288 (Figure 4). The higher expression of *MAPK*s (and *MAP2K*s and *MAP3K*s) during early infection hours in ZYM1288 is quite relatable to their downstream presence of pathogen sensors/receptors [44]. Furthermore, the differential regulation of *NDPK*s, *ANP1*, *PRP*s, *MAPK*, *MAP2K*, and *MAP3K*s in both genotypes indicate the possibility that that hulless barley, after PM attack, prepares for cell death and/or H_2O_2 production, accumulation of reactive oxygen species, and activates defense related proteins [47]. We discussed in the above section that JA might also be playing role in defense responses against PM in ZYM1288. In this regard, the increased expression of *CHI-B*s, *ERF1*s, and *VIP2* (along with *MYC2*s) in ZYM1288 is possibly generating wounding as well as defense responses through the cross-talk between ethylene and JA signaling [48]. Taken together, it can be suggested that the MAPK signaling pathway is one of the defense strategies that is general to hulless barley genotypes to send downstream signals for defense responses. Relatively higher expression of key genes in MAPK signaling pathway might be enabling ZYM1288 to show higher resistance to PM. Further, the results showed that triggering toll-like receptor kinase signaling pathway related genes (especially a higher number of *IRAK1*s and *IRAK4*s) is possibly a common response to PM in hulless barley. This proposition is based on the observation of variable expression of these genes in both studied genotypes (Supplementary Table S2). It is known that these receptor like kinases act as a bridge between PM signals and intracellular regulatory machinery in plants [49].

3.3. PM Infection Modulates Changes in Energy Related Pathways in Hulless Barley

Powdery mildew infection significantly affects the photosynthesis and subsequent energy related processes [50]. One of the reasons for the increasing leaf yellowing with the time in XL19 is possibly due to the reduced expression of *lhc1* (*HOVUSG0250900*) as compared to ZYM1288, meaning that the capture and delivery of the excitation energy to PSI in XL19 was reduced [51]. Further, the downregulation of relatively higher number of photosynthesis associated proteins (photosystem II (PSII) proteins and *ferredoxin* proteins) in XL19 reduced its photosynthetic potential that possibly affected downstream energy metabolism related pathways [52,53]. The slight yellowing noticed in ZYM1288 at latter time points (36 hpi) is possibly because of the downregulation of *ferredoxin-NADP+ reductase*, *P680 D1*, and a *PSII 10 kDa* protein (Supplementary Table S3). Thus, PM affects photosynthesis and photosynthesis-antenna proteins in hulless barley regardless of the genetic background but the resistant genotype showed higher expression of related genes, particularly at early infection stages [54]. PM also affected the downstream pathways i.e., carbon fixation in photosynthetic organisms, nitrogen metabolism, citrate cycle, and starch and sucrose metabolism in both genotypes. These changes are consistent with the findings that PM infection significantly impaired the tricarboxylic acid cycle, electron transfer capacity, photochemical efficiency in rubber tree [55]. These transcriptomic signatures are complex and should be explored with a specific focus on their role in defense against PM in barley. Previously, it is known that PM infection significantly alters the CO_2 fixation and light utilization in sugar beet leaves [56]. Possibly, the PM is affecting hulless barley leaves similarly, since both genotypes exhibited differential regulation of the key enzymes (*MDH*,

*PEP, ALDOA*s, *AS,* and *RBCS*s) [57–59]. Such changes at biochemical level have also been reported in rubber tree [55].

3.4. PM Triggers Changes in Defense-Associated Pathways in Hulless Barley

The plant-pathogen interaction pathway is the major pathway associated with defense mechanisms in plants is [60]. CDPKs are present in cytoplasm which (along with *CNGC*s, *CML*s, *NOS*, and *RBO*s) execute PTI and develop the HR and reinforce cell wall (and stomatal closure) [61]. In addition to these roles, the CKPKs in barley have been shown to antagonistically control the entry of PM into the host cell [62]. Therefore, the differential expression of CDPKs in both genotypes indicated that hulless barley uses HR to PM infection. However, the upregulation of multiple genes in these key stages of HR in ZYM1288 like *CML*s, *CNGC*, and *NOS* enabled this genotype for better resistance against invading PM (Figure 5). Further, HR is also driven by ETI in which *RIN*s, *RPM*s, and *RPS*s effect SGT1, HSP90, and RAR1 [63]. The effector triggered genes, i.e., *RIN*s, *RPM*s, and *RPS*s, were differentially expressed in both genotypes, indicating that hulless barley also relies on these genes for resistance against PM. However, upregulation of *HSP90* in ZYM1288 could be another reason for enhanced resistance to PM.

Apart from the PTI and ETI, several other pathways such as brassinosteroid biosynthesis, glutathione metabolism, and glucosinolate metabolism are essential defense strategies in plants [64–66]. The higher expression of *T9L24.44*, *BR6-COX1*, *CYP724B1*s, *BAS*1, and *CYP92A6*s in ZYM1288 must have increased the brassinosteroid levels that led to resistance to PM. This is supported by the known function of these genes in brassinosteroid biosynthesis and the fact that brassinosteroids defend plants against broad range of diseases, particularly against the virulent PM *Odium* sp. in tobacco [67]. Furthermore, the upregulation of two *BRI1s* in ZYM1288 is also in agreement with the results of an earlier study that brassinosteroid led increased resistance in uzu barley lines [67]. In addition to brassinosteroids, studies in other plants have highlighted the role of glutathione in plant signaling and ultimately defense responses against biotic stresses [68]. The differential expression of DEGs related to this pathway in the leaf transcriptome of XL19 and ZYM1288 suggests that PM infection triggers changes in glutathione metabolism in hulless barley. Particularly, the upregulation of *GST*s is consistent with the previous findings that PM infection induced higher transcripts of *GstA1* gene in barley and it was suggested that it mainly prevents plant cell disruption and death by PM [69]. However, other studies identified that *GST* activity can be variable in resistant and susceptible genotypes, which is consistent with our results [70,71]. Apart from these two pathways, the large-scale transcriptomic changes in secondary metabolite biosynthesis indicates that secondary metabolites may also play important roles in resistance to PM. This in agreement with the transcriptome level studies in wheat, barley, grapevine, *Vitis pseudoreticulata*, *Fragaria vesca*, pumpkin, and melon [19,20,72–74]. Secondary metabolites play diverse roles in plant innate immunity and the differential regulation of this pathway in both hulless barley genotypes is indicative of diverse role of this pathway against resistance to PM (Supplementary Table S3).

3.5. XL19 and ZYM1288 Differ in the Expression of Known PM Resistance Loci/Genes

In barley, the control of *Bgh* is associated with many resistance-related loci. The comparative transcriptome of both genotypes suggested the presence of both *Mlo* and *Mla* loci. The resistance of ZYM1288, based on leaf transcriptome, is possibly due to the downregulation of the *Mlo* genes and the upregulation of *Mla* genes. This is quite understandable since the knockdown of *Mlo* genes in grapevine reduces the susceptibility to PM, thus, the relative upregulation of these genes in XL19 made this genotype susceptible. Contrastingly, the *Mla* locus in barley gives isolate-specific immunity to PM [75], thus the ZYM1288 is a PM resistant genotype. Apart from these loci, it is known that *SNARE*-dependent antimicrobial secretion pathway limits the PM penetration [76], including different *SNARE* proteins (including *SYP*s) [77]. The upregulation of two *SYP*s (*syntaxin 1B/2/3*) in ZYM1288 suggested their role in limiting the *Bgh* penetration. On the other hand, in XL19, its down-

regulation as compared to ZYM1288 is possibly due to the fact that syntaxin-dependent exocytosis is required for *mlo*-based defense as observed previously [78,79]. Another known regulator of barley defense against PM is the *SKP1*, that controls the abundance of PM susceptibility factor (RACB) [80]. This gene was active in both genotypes since its differential expression was modulated contrastingly in XL19 as well as ZYM1288 (Figure 7). Apart from the possible roles of these genes in resistance to PM, the resistance in ZYM1288 can also be explained by the high upregulation of *PLSC* gene (Figure 7) since a recent study reported glycerol-mediated PM resistance due to increased expressed on glycerol 3-phosphate [81]. The upregulation of inversins also increased PM resistance in ZYM1288 as soybean transgenic lines containing ankyrin-repeat containing gene exhibited enhanced resistance to fungus (*Fusarium virguiforme*) [81].

4. Conclusions

In this study, we compared the phytohormone levels and the transcriptome of two hulless barley genotypes with contrasting resistance to PM. ZYM1288 genotype was resistant to PM due to increased levels of defense related phytohormones i.e., ABA, SA, and JA. These increased levels in ZYM1288 triggered downstream phytohormone signaling cascade as noticed by the upregulation of genes such as *ABI5*, *TIFYs*, *MYC2*s, *JAR1*, and *CLIKE3*, and PRP. The JA signaling as a part of MAPK signaling pathway possibly induced wounding and defense responses. The PM infection triggered the MAPK signaling pathway, toll-like receptor kinase signaling, and plant-pathogen interaction pathways. Infection with *Bgh* modulated changes in the important energy related pathways. Genes related to both ETI and PTI were expressed in both ZYM1288 and XL19, however, increased expression of major genes in ZYM1288 possibly governed resistance to PM. Expression of brassinosteroid biosynthesis related genes was increased in ZYM1288, while the glutathione, glucosinolate, and secondary metabolite biosynthesis pathways showed variable expression patterns at different key steps of each pathway. The susceptibility of XL19 is indicated by the higher expression of *Mlo* genes, lower expression of *Mla* genes as compared to ZYM1288. The upregulation of *Mla,* syntaxin, and *PLSC* together with the regulation of brassinosteroid pathway, energy related pathways, signaling pathways, and plant-pathogen interaction pathway gave higher *Bgh* resistance potential to ZYM1288. The transcriptomic signatures identified in ZYM1288 are an important basis for future breeding of hulless barley for increased resistance against PM.

5. Material and Method

5.1. Plant Materials, Growth Conditions, and Inoculation

Two hulless barley genotypes whose contrasting resistance levels to PM (*Blumeria graminis*) f. sp. *Hordei* (*Bgh*) i.e., susceptible variety Xila 19 (XL19) and resistant variety ZYM1288 were identified in a separate study at the Agricultural Research Institute of the Academy of Agricultural and Animal Husbandry of the Tibet Autonomous Region, China. Seeds were grown in plastic flowerpots (8 cm diameter) in a greenhouse at 22 °C temperature and a photoperiod of 12 h. The pathogen infected samples were collected from a local field and maintained on susceptible variety XL19 in the greenhouse. Humidity, temperature, and photoperiod for pathogen infected samples were maintained at 70%, 22/18 °C, and 14 h light/10 h darkness, respectively. When both XL19 and ZYM1288 seedlings reached two-leaf and one heart stage, they were infected with the *Bgh* as reported earlier [2], and the leaf samples were harvested at four time points i.e., 5, 12, 24, and 36 h, and control (CK, 0 h; the non-infected plants were considered as 0 h post infection (hpi)). The *Bgh* isolate was maintained on a susceptible hulless barley cultivar Z13 at Agricultural Research Institute of the Academy of Agricultural and Animal Husbandry of the Tibet Autonomous Region, China. Three biological replicates were collected for each time point and variety for phytohormone and transcriptome analyses.

5.2. Phytohormone Detection

Phytohormones were detected by MetWare (http://www.metware.cn/, accessed on 2 February 2020) based on the AB Sciex QTRAP 6500 LC-MS/MS platform. Briefly, 50 mg fresh weight of leaves per replicate for each variety were ground into powder in liquid nitrogen and extracted with methanol/water/formic acid ($V/V/V$, 15:4:1). The extracts were then dried by evaporating under nitrogen gas stream, followed by the addition of 80% methanol (V/V), and filtration through a 0.22 μm PFTE membrane filter. The filtrate was then subjected to LC-MS/S analyses as described previously [9,82].

5.3. Transcriptome Sequencing, Data Analyses, Differential Gene Expression, and Enrichment Analyses

Total RNA was extracted from each biological replicate of XL19 and ZYM1288 and after checking its purity, it was quantified and integrity was tested. The cDNA was synthesized, libraries were prepared, and sequenced on Illumina HiSeq platform (Illumina Inc., San Diego, CA, USA) at MetWare (http://www.metware.cn/, accessed on 2 February 2020). The methods for cDNA synthesis, library construction, and sequencing were adopted from previous reports [83].

FastQC was used for quality assessing and obtaining clean reads followed by checking the GC content distribution (http://www.bioinformatics.babraham.ac.uk/projects/fastqc/, accessed on 2 February 2020). The clean reads were stitched in Trinity [84] and compared to the reference genome [22,85] using HISAT2 [86] and the proportion of generated sequence reads that were aligned to the reference genome as calculated as total mapped reads/fragments.

The gene expression was quantified as Fragments Per Kilobase of transcript per Million Fragments Mapped (FPKM) [87]. The Pearson Correlation Coefficient (PCC) was estimated between the expression of biological replicates [83]. Differentially expressed genes (DEGs) between XL19 and ZYM1288 treatments were identified by using DESeq2 [88] by normalizing the read counts in featureCounts [89]. We used fold change (FC) ≥ 1 [90] and FDR correction set at $p < 0.05$ as screening conditions. Venn diagrams of DEGs were prepared in InteractiVenn [91].

The DEGs were annotated in different databases such as Kyoto Encyclopedia of Genes and Genomes (KEGG) [92], Gene Ontology (GO) [93], Clusters of Orthologous Groups (COG) [94], PfAM, Swissprot [95], Eukaryotic Orthologous Groups of proteins (KOG) [96] databases. To determine the gene expression, we compared the sequenced reads with the unigene library in Bowtie [97], and Fragments Per Kilobase of transcript per Million Fragments Mapped (FPKM) was estimated in combination with featureCounts (1.6.1) [89]. KEGG pathway enrichment of DEGs was done by using KOBAS2.0 and FDR correction ($p < 0.05$) was used to reduce false positive prediction [98]. The DEGs for specific pathway were filtered based on annotations and enrichment analyses and heatmaps were prepared in TBtools [99].

5.4. qRT-PCR Analysis of Selected DEGs

The expression of seven genes that were differentially expressed in response to *Bgh* infection in XL19 and ZYM was quantified by QRT-PCR to check the reliability of the RNA-Seq results. The primers used for analysis are listed in Table 1. *GAPDH* gene [100] was used as an internal control. The analysis was performed using applied Biosystems StepOnePlus[TM] Real-Time System (Applied Biosystems, Waltham, MS, USA). SYBR[®] Select Master Mix (2X) was used for reactions. The reaction conditions were 90 °C for 10 min followed by 40 cycles of denaturation, annealing, and extension. Each reaction included denaturation at 90 °C for 10 s, annealing at 60 °C for 60 s, and extension at 72 °C for 30 s. The relative expression of each gene was calculated using $2^{(-\triangle\triangle CT)}$ method. The values of the relative expression were used to calculate mean and standard deviation in Microsoft Excel 2019[®]. Furthermore, we also determined the correlation (R^2) between the RT-PCR expression data and RNA-seq data in R.

Table 1. List of primers used for quantitative real-time PCR analysis of selected DEGs.

Gene	Primers
GAPDH	F-CTAAGTTTTTGGGTGT R-CTATGAATTGGTCTTCC
HOVUSG4120900	F-GGCACCTCCAAGCACCAGAT R-ACACCCGAACCAAAGTAGCG
HOVUSG6135200	F-CTTTTGGGAGAACGATGGA R-TGTTTGGTAGGTGCTCTTTATG
HOVUSG0289600	F-TAATCTATTGGATGACACTGGGA R-CTGTGAGAGGCTTTGCTTGA
HOVUSG2614500	F-CGCATTTGTCGCAAAACA R-GATGAGCGTGCCAACCC
HOVUSG2888400	F-GGGTCCTTGTCTGCCTGG R-CGCTCTGTTTCTTGCTTCC
HOVUSG3967100	F-GGATGAAGGGGAAGACGG R-ACAGAGGGTCGGCGGAGA
HOVUSG2306000	F-TCAGTGCGGTAGAGCGAGC R-GGTGACGCCGAGGATGGG

Abbreviations

ABA	Abscisic acid
ABI5	ABA-insensitive 5
ALDOA	Fructose-bisphosphate aldolases
APXs	L-ascorbate peroxidases
AST	Aspartate aminotransferase
AUX	Auxin induced proteins
Bgh	*Blumeria graminis* (DC.) Golovin ex Speer f. sp. hordei Marchal
CDPK	Calcium Depedent Protein Kinase
COG	Clusters of Orthologous Groups
DEGs	Differentially expressed genes
ETI	Effector triggered immunity
FPKM	Fragments Per Kilobase of Transcript per Million fragments mapped
GGCTs	Gamma-glutamylcyclotransferase-plant
GO	Gene Ontology
GSS	Glutathione synthase
GSTs	Glutathione s-transferases
H2JA	Dihydrojasmonic acid
HK	Histidine kinases
HR	Hypersensitive response
IAA	Indole 3-acetic acid
ICA	Indole-3-carboxylic acid
ICA-Id	Indole-3-carboxaldehyde
IDH	Isocitrate dehydrogenase
iPPase	inorganic pyrophosphatases
IRAK	Interleukin-1 receptor-associated kinases
JA	Jasmonic acid
JA-ILE	Jasmonoyl-L-Isoleucine
KEGG	Kyoto Encyclopedia of Genes and Genomes
KOG	Eukaryotic Orthologous Groups of proteins
LAPs	Leucyl aminopeptidases
MAPK	Mitogen-activated protein kinase
MDH	Malate dehydrogenase
MEIAA	Methylindole-3-acetic acid
MEJA	Methyl Jasmonate
Mlo	MILDEW RESISTANCE LOCUS O
MRPs	Multidrug resistance proteins
ORRs	Two-component response regulations
PAMP	Pathogen-associated molecular patterns
PCC	Pearson Correlation Coefficient
PEN	PENETRATION proteins
6PGD	6-phosphogluconate dehydrogenase
PEP	Phosphoenolpyruvate carboxylase
PHP5	Phosphotransfer protein 5
PLSC	1-acyl-sn-glycerol-3-phosphate acyltransferase
PM	Powdery mildew
PP2A	Serine/threonine-protein phosphatase 2A activator
PRMC	Release factor glutamine methyltransferase
PS	Photosystem
PTI	PAMP-triggered immunity
RGA	Disease resistance gene analogs
RRM1s	Ribonucleoside-diphosphate reductase subunit M1
RRM2	cold-inducible RNA-binding protein
SA	Salicylic acid

SGT1	Suppressor of the G2 allele of skp1
SKP1	S-phase kinase-associated protein 1
SYP	SYNTAXIN OF PLANTS
T9L24.4	Steroid 22-alpha-hydroxylase
TUBGCP6	Gamma-tubulin complex component 6
tZ	trans-zeatin

References

1. Zha, S.; Yang, C.; Zeng, X.; Li, Z.; Wang, Y.; Yuan, H.; Yu, M.; Xu, Q. Comparative analysis of H3K4 and H3K27 trimethylations in two contrasting Tibetan hulless barely varieties on powdery mildew infection. *J. Plant Pathol.* **2021**, *103*, 117–126. [CrossRef]
2. Yuan, H.; Zeng, X.; Yang, Q.; Xu, Q.; Wang, Y.; Jabu, D.; Sang, Z.; Tashi, N. Gene coexpression network analysis combined with metabonomics reveals the resistance responses to powdery mildew in Tibetan hulless barley. *Sci. Rep.* **2018**, *8*, 1–13. [CrossRef] [PubMed]
3. Dreiseitl, A.; Yang, J. Powdery mildew resistance in a collection of Chinese barley varieties. *Genet. Resour. Crop Evol.* **2007**, *54*, 259–266. [CrossRef]
4. Cao, X.-R.; Yao, D.-M.; Duan, X.-Y.; Wei, L.; Fan, J.-R.; Ding, K.-J.; Zhou, Y.-L. Effects of powdery mildew on 1000-kernel weight, crude protein content and yield of winter wheat in three consecutive growing seasons. *J. Integr. Agric.* **2014**, *13*, 1530–1537. [CrossRef]
5. Zhou, M. Barley production and consumption. In *Genetics and Improvement of Barley Malt Quality*; Springer: Berlin/Heidelberg, Germany, 2009; pp. 1–17.
6. Ridout, C.J.; Skamnioti, P.; Porritt, O.; Sacristan, S.; Jones, J.D.; Brown, J.K. Multiple avirulence paralogues in cereal powdery mildew fungi may contribute to parasite fitness and defeat of plant resistance. *Plant Cell* **2006**, *18*, 2402–2414. [CrossRef]
7. Ramos, S.M.B.; Almeida, E.F.A.; Rocha, F.d.S.; Fernandes, M.d.F.G.; Santos, E.B.d. Organic fertilization and alternative products in the control of powdery mildew. *Ornam. Hortic.* **2020**, *26*, 57–68. [CrossRef]
8. Zubrod, J.P.; Bundschuh, M.; Arts, G.; Brühl, C.A.; Imfeld, G.; Knäbel, A.; Payraudeau, S.; Rasmussen, J.J.; Rohr, J.; Scharmüller, A. Fungicides: An overlooked pesticide class? *Environ. Sci. Technol.* **2019**, *53*, 3347–3365. [CrossRef]
9. Yang, F.; Yang, T.; Liu, K.; Yang, Q.; Wan, Y.; Wang, R.; Li, G. Analysis of Metabolite Accumulation Related to Pod Color Variation of Caragana intermedia. *Molecules* **2019**, *24*, 717. [CrossRef]
10. Jones, J.D.; Dangl, J.L. The plant immune system. *Nature* **2006**, *444*, 323–329. [CrossRef] [PubMed]
11. Chelkowski, J.; Tyrka, M.; Sobkiewicz, A. Resistance genes in barley (*Hordeum vulgare* L.) and their identification with molecular markers. *J. Appl. Genet.* **2003**, *44*, 291–310.
12. Piechota, U.; Czembor, P.C.; Słowacki, P.; Czembor, J.H. Identifying a novel powdery mildew resistance gene in a barley landrace from Morocco. *J. Appl. Genet.* **2019**, *60*, 243–254. [CrossRef] [PubMed]
13. Lu, X.; Kracher, B.; Saur, I.M.; Bauer, S.; Ellwood, S.R.; Wise, R.; Yaeno, T.; Maekawa, T.; Schulze-Lefert, P. Allelic barley MLA immune receptors recognize sequence-unrelated avirulence effectors of the powdery mildew pathogen. *Proc. Natl. Acad. Sci. USA* **2016**, *113*, E6486–E6495. [CrossRef]
14. Ge, X.; Deng, W.; Lee, Z.Z.; Lopez-Ruiz, F.J.; Schweizer, P.; Ellwood, S.R. Tempered mlo broad-spectrum resistance to barley powdery mildew in an Ethiopian landrace. *Sci. Rep.* **2016**, *6*, 29558. [CrossRef] [PubMed]
15. Kuhn, H.; Lorek, J.; Kwaaitaal, M.; Consonni, C.; Becker, K.; Micali, C.; Ver Loren van Themaat, E.; Bednarek, P.; Raaymakers, T.M.; Appiano, M. Key components of different plant defense pathways are dispensable for powdery mildew resistance of the Arabidopsis mlo2 mlo6 mlo12 triple mutant. *Front. Plant Sci.* **2017**, *8*, 1006. [CrossRef] [PubMed]
16. Jia, M.; Xu, H.; Liu, C.; Mao, R.; Li, H.; Liu, J.; Du, W.; Wang, W.; Zhang, X.; Han, R. Characterization of the powdery mildew resistance gene in the elite wheat cultivar Jimai 23 and its application in marker-assisted selection. *Front. Genet.* **2020**, *11*, 241. [CrossRef]
17. Li, H.; Dong, Z.; Ma, C.; Tian, X.; Xiang, Z.; Xia, Q.; Ma, P.; Liu, W. Discovery of powdery mildew resistance gene candidates from Aegilops biuncialis chromosome 2Mb based on transcriptome sequencing. *PLoS ONE* **2019**, *14*, e0220089. [CrossRef]
18. Li, Y.; Guo, G.; Zhou, L.; Chen, Y.; Zong, Y.; Huang, J.; Lu, R.; Liu, C. Transcriptome Analysis Identifies Candidate Genes and Functional Pathways Controlling the Response of Two Contrasting Barley Varieties to Powdery Mildew Infection. *Int. J. Mol. Sci.* **2020**, *21*, 151. [CrossRef]
19. Xin, M.; Wang, X.; Peng, H.; Yao, Y.; Xie, C.; Han, Y.; Ni, Z.; Sun, Q. Transcriptome comparison of susceptible and resistant wheat in response to powdery mildew infection. *Genom. Proteom. Bioinform.* **2012**, *10*, 94–106. [CrossRef]
20. Zhu, Q.; Gao, P.; Wan, Y.; Cui, H.; Fan, C.; Liu, S.; Luan, F. Comparative transcriptome profiling of genes and pathways related to resistance against powdery mildew in two contrasting melon genotypes. *Sci. Hortic.* **2018**, *227*, 169–180. [CrossRef]
21. Saja, D.; Janeczko, A.; Barna, B.; Skoczowski, A.; Dziurka, M.; Kornaś, A.; Gullner, G. Powdery Mildew-Induced Hormonal and Photosynthetic Changes in Barley Near Isogenic Lines Carrying Various Resistant Genes. *Int. J. Mol. Sci.* **2020**, *21*, 4536. [CrossRef]
22. Zeng, X.; Xu, T.; Ling, Z.; Wang, Y.; Li, X.; Xu, S.; Xu, Q.; Zha, S.; Qimei, W.; Basang, Y.; et al. An improved high-quality genome assembly and annotation of Tibetan hulless barley. *Sci. Data* **2020**, *7*, 1–9. [CrossRef]

23. Guo, W.-L.; Chen, B.-H.; Chen, X.-J.; Guo, Y.-Y.; Yang, H.-L.; Li, X.-Z.; Wang, G.-Y. Transcriptome profiling of pumpkin (Cucurbita moschata Duch.) leaves infected with powdery mildew. *PLoS ONE* **2018**, *13*, e0190175. [CrossRef] [PubMed]

24. Bari, R.; Jones, J.D. Role of plant hormones in plant defence responses. *Plant Mol. Biol.* **2009**, *69*, 473–488. [CrossRef] [PubMed]

25. Li, R.; Zhang, L.-L.; Yang, X.-M.; Cao, X.-L.; Wang, Y.-G.; Ma, X.-F.; Chandran, V.; Fan, J.; Yang, H.; Shang, J. Transcriptome analysis reveals pathways facilitating the growth of tobacco powdery mildew in Arabidopsis. *Phytopathol. Res.* **2019**, *1*, 7. [CrossRef]

26. Tian, X.; Zhang, L.; Feng, S.; Zhao, Z.; Wang, X.; Gao, H. Transcriptome analysis of apple leaves in response to powdery mildew (*Podosphaera leucotricha*) infection. *Int. J. Mol. Sci.* **2019**, *20*, 2326. [CrossRef] [PubMed]

27. Fung, R.W.; Gonzalo, M.; Fekete, C.; Kovacs, L.G.; He, Y.; Marsh, E.; McIntyre, L.M.; Schachtman, D.P.; Qiu, W. Powdery mildew induces defense-oriented reprogramming of the transcriptome in a susceptible but not in a resistant grapevine. *Plant Physiol.* **2008**, *146*, 236–249. [CrossRef] [PubMed]

28. Bilgin, D.D.; Zavala, J.A.; Zhu, J.; Clough, S.J.; Ort, D.R.; DeLUCIA, E.H. Biotic stress globally downregulates photosynthesis genes. *Plant Cell Environ.* **2010**, *33*, 1597–1613. [CrossRef]

29. Lyu, X.; Shen, C.; Xie, J.; Fu, Y.; Jiang, D.; Hu, Z.; Tang, L.; Tang, L.; Ding, F.; Li, K. A "footprint" of plant carbon fixation cycle functions during the development of a heterotrophic fungus. *Sci. Rep.* **2015**, *5*, 1–13. [CrossRef]

30. Tanabe, S.; Ashikari, M.; Fujioka, S.; Takatsuto, S.; Yoshida, S.; Yano, M.; Yoshimura, A.; Kitano, H.; Matsuoka, M.; Fujisawa, Y. A novel cytochrome P450 is implicated in brassinosteroid biosynthesis via the characterization of a rice dwarf mutant, dwarf11, with reduced seed length. *Plant Cell* **2005**, *17*, 776–790. [CrossRef]

31. Kang, J.-G.; Yun, J.; Kim, D.-H.; Chung, K.-S.; Fujioka, S.; Kim, J.-I.; Dae, H.-W.; Yoshida, S.; Takatsuto, S.; Song, P.-S. Light and brassinosteroid signals are integrated via a dark-induced small G protein in etiolated seedling growth. *Cell* **2001**, *105*, 625–636. [CrossRef]

32. Ali, S.S.; Gunupuru, L.R.; Kumar, G.S.; Khan, M.; Scofield, S.; Nicholson, P.; Doohan, F.M. Plant disease resistance is augmented in uzu barley lines modified in the brassinosteroid receptor BRI1. *BMC Plant Biol.* **2014**, *14*, 227. [CrossRef]

33. Singh, A. Glucosinolates and Plant Defense. In *Glucosinolates*; Mérillon, J.M., Ramawat, K.G., Eds.; Springer: Berlin/Heidelberg, Germany, 2017; pp. 237–246.

34. Ghanashyam, C.; Jain, M. Role of auxin-responsive genes in biotic stress responses. *Plant Signal. Behav.* **2009**, *4*, 846–848. [CrossRef]

35. Spartz, A.K.; Ren, H.; Park, M.Y.; Grandt, K.N.; Lee, S.H.; Murphy, A.S.; Sussman, M.R.; Overvoorde, P.J.; Gray, W.M. SAUR inhibition of PP2C-D phosphatases activates plasma membrane H+-ATPases to promote cell expansion in Arabidopsis. *Plant Cell* **2014**, *26*, 2129–2142. [CrossRef]

36. Gupta, R.; Pizarro, L.; Leibman-Markus, M.; Marash, I.; Bar, M. Cytokinin response induces immunity and fungal pathogen resistance, and modulates trafficking of the PRR LeEIX2 in tomato. *Mol. Plant Pathol.* **2020**, *21*, 1287–1306. [CrossRef] [PubMed]

37. Pham, J.; Liu, J.; Bennett, M.H.; Mansfield, J.W.; Desikan, R. Arabidopsis histidine kinase 5 regulates salt sensitivity and resistance against bacterial and fungal infection. *New Phytol.* **2012**, *194*, 168–180. [CrossRef] [PubMed]

38. Hutchison, C.E.; Li, J.; Argueso, C.; Gonzalez, M.; Lee, E.; Lewis, M.W.; Maxwell, B.B.; Perdue, T.D.; Schaller, G.E.; Alonso, J.M. The Arabidopsis histidine phosphotransfer proteins are redundant positive regulators of cytokinin signaling. *Plant Cell* **2006**, *18*, 3073–3087. [CrossRef]

39. Argueso, C.T.; Ferreira, F.J.; Epple, P.; To, J.P.; Hutchison, C.E.; Schaller, G.E.; Dangl, J.L.; Kieber, J.J. Two-component elements mediate interactions between cytokinin and salicylic acid in plant immunity. *PLoS Genet.* **2012**, *8*, e1002448. [CrossRef]

40. Han, X.; Kahmann, R. Manipulation of phytohormone pathways by effectors of filamentous plant pathogens. *Front. Plant Sci.* **2019**, *10*, 822. [CrossRef] [PubMed]

41. Brocard, I.M.; Lynch, T.J.; Finkelstein, R.R. Regulation and role of the Arabidopsis abscisic acid-insensitive 5 gene in abscisic acid, sugar, and stress response. *Plant Physiol.* **2002**, *129*, 1533–1543. [CrossRef]

42. Guerreiro, A.; Figueiredo, J.; Sousa Silva, M.; Figueiredo, A. Linking jasmonic acid to grapevine resistance against the biotrophic oomycete Plasmopara viticola. *Front. Plant Sci.* **2016**, *7*, 565. [CrossRef]

43. Shah, J. The salicylic acid loop in plant defense. *Curr. Opin. Plant Biol.* **2003**, *6*, 365–371. [CrossRef]

44. Meng, X.; Zhang, S. MAPK cascades in plant disease resistance signaling. *Annu. Rev. Phytopathol.* **2013**, *51*, 245–266. [CrossRef] [PubMed]

45. Pedley, K.F.; Martin, G.B. Role of mitogen-activated protein kinases in plant immunity. *Curr. Opin. Plant Biol.* **2005**, *8*, 541–547. [CrossRef] [PubMed]

46. Shi, H.; Yan, H.; Li, J.; Tang, D. BSK1, a receptor-like cytoplasmic kinase, involved in both BR signaling and innate immunity in Arabidopsis. *Plant Signal. Behav.* **2013**, *8*, e24996. [CrossRef] [PubMed]

47. Liu, Y.; He, C. A review of redox signaling and the control of MAP kinase pathway in plants. *Redox Biol.* **2017**, *11*, 192–204. [CrossRef] [PubMed]

48. Lorenzo, O.; Piqueras, R.; Sánchez-Serrano, J.J.; Solano, R. ETHYLENE RESPONSE FACTOR1 integrates signals from ethylene and jasmonate pathways in plant defense. *Plant Cell* **2003**, *15*, 165–178. [CrossRef] [PubMed]

49. Jose, J.; Ghantasala, S.; Roy Choudhury, S. Arabidopsis Transmembrane Receptor-Like Kinases (RLKs): A Bridge between Extracellular Signal and Intracellular Regulatory Machinery. *Int. J. Mol. Sci.* **2020**, *21*, 4000. [CrossRef] [PubMed]

50. Magyarosy, A.C.; Schürmann, P.; Buchanan, B.B. Effect of powdery mildew infection on photosynthesis by leaves and chloroplasts of sugar beets. *Plant Physiol.* **1976**, *57*, 486–489. [CrossRef]

51. Wientjes, E.; van Stokkum, I.H.; van Amerongen, H.; Croce, R. The role of the individual Lhcas in photosystem I excitation energy trapping. *Biophys. J.* **2011**, *101*, 745–754. [CrossRef] [PubMed]

52. Zeng, X.-Q.; Luo, X.-M.; Wang, Y.-L.; Xu, Q.-J.; Bai, L.-J.; Yuan, H.-J.; Tashi, N. Transcriptome sequencing in a Tibetan barley landrace with high resistance to powdery mildew. *Sci. World J.* **2014**, *2014*, 594579. [CrossRef] [PubMed]

53. Zhang, H.; Chen, Y.; Niu, Y.; Zhang, X.; Zhao, J.; Sun, L.; Wang, H.; Xiao, J.; Wang, X. Characterization and fine mapping of a leaf yellowing mutant in common wheat. *Plant Growth Regul.* **2020**, *92*, 233–247. [CrossRef]

54. Hu, Y.; Zhong, S.; Zhang, M.; Liang, Y.; Gong, G.; Chang, X.; Tan, F.; Yang, H.; Qiu, X.; Luo, L. Potential Role of Photosynthesis in the Regulation of Reactive Oxygen Species and Defence Responses to *Blumeria graminis* f. sp. tritici in Wheat. *Int. J. Mol. Sci.* **2020**, *21*, 5767. [CrossRef]

55. Wang, L.-F.; Wang, M.; Zhang, Y. Effects of powdery mildew infection on chloroplast and mitochondrial functions in rubber tree. *Trop. Plant Pathol.* **2014**, *39*, 242–250. [CrossRef]

56. Gordon, T.R.; Duniway, J.M. Effects of powdery mildew infection on the efficiency of CO_2 fixation and light utilization by sugar beet leaves. *Plant Physiol.* **1982**, *69*, 139–142. [CrossRef]

57. Uematsu, K.; Suzuki, N.; Iwamae, T.; Inui, M.; Yukawa, H. Increased fructose 1, 6-bisphosphate aldolase in plastids enhances growth and photosynthesis of tobacco plants. *J. Exp. Bot.* **2012**, *63*, 3001–3009. [CrossRef]

58. Nunes-Nesi, A.; Carrari, F.; Lytovchenko, A.; Smith, A.M.; Loureiro, M.E.; Ratcliffe, R.G.; Sweetlove, L.J.; Fernie, A.R. Enhanced photosynthetic performance and growth as a consequence of decreasing mitochondrial malate dehydrogenase activity in transgenic tomato plants. *Plant Physiol.* **2005**, *137*, 611–622. [CrossRef] [PubMed]

59. Suh, S.W.; Cascio, D.; Chapman, M.S.; Eisenberg, D. A crystal form of ribulose-1, 5-bisphosphate carboxylase/oxygenase from Nicotiana tabacum in the activated state. *J. Mol. Biol.* **1987**, *197*, 363–365. [CrossRef]

60. Staskawicz, B.J. Genetics of plant-pathogen interactions specifying plant disease resistance. *Plant Physiol.* **2001**, *125*, 73–76. [CrossRef] [PubMed]

61. Zhang, J.; Zhou, J.-M. Plant immunity triggered by microbial molecular signatures. *Mol. Plant* **2010**, *3*, 783–793. [CrossRef] [PubMed]

62. Li, A.; Wang, X.; Leseberg, C.H.; Jia, J.; Mao, L. Biotic and abiotic stress responses through calcium-dependent protein kinase (CDPK) signaling in wheat (*Triticum aestivum* L.). *Plant Signal. Behav.* **2008**, *3*, 654–656. [CrossRef]

63. Seo, Y.-S.; Lee, S.-K.; Song, M.-Y.; Suh, J.-P.; Hahn, T.-R.; Ronald, P.; Jeon, J.-S. The HSP90-SGT1-RAR1 molecular chaperone complex: A core modulator in plant immunity. *J. Plant Biol.* **2008**, *51*, 1–10. [CrossRef]

64. Wang, Z.-Y. Brassinosteroids modulate plant immunity at multiple levels. *Proc. Natl. Acad. Sci. USA* **2012**, *109*, 7–8. [CrossRef]

65. Radojčić Redovniković, I.; Glivetić, T.; Delonga, K.; Vorkapić-Furač, J. Glucosinolates and their potential role in plant. *Period. Biol.* **2008**, *110*, 297–309.

66. Gullner, G.; Kömives, T. The role of glutathione and glutathione-related enzymes in plant-pathogen interactions. In *Significance of Glutathione to Plant Adaptation to the Environment*; Springer: Berlin/Heidelberg, Germany, 2001; pp. 207–239.

67. Nakashita, H.; Yasuda, M.; Nitta, T.; Asami, T.; Fujioka, S.; Arai, Y.; Sekimata, K.; Takatsuto, S.; Yamaguchi, I.; Yoshida, S. Brassinosteroid functions in a broad range of disease resistance in tobacco and rice. *Plant J.* **2003**, *33*, 887–898. [CrossRef] [PubMed]

68. Dubreuil-Maurizi, C.; Poinssot, B. Role of glutathione in plant signaling under biotic stress. *Plant Signal. Behav.* **2012**, *7*, 210–212. [CrossRef] [PubMed]

69. El Zahaby, H.; Gullner, G.; Kiraly, Z. Effects of powdery mildew infection of barley on the ascorbate-glutathione cycle and other antioxidants in different host-pathogen interactions. *Phytopathology* **1995**, *85*, 1225–1230. [CrossRef]

70. Gullner, G.; Komives, T.; Király, L.; Schröder, P. Glutathione S-transferase enzymes in plant-pathogen interactions. *Front. Plant Sci.* **2018**, *9*, 1836. [CrossRef]

71. Harrach, B.D.; Fodor, J.; Pogány, M.; Preuss, J.; Barna, B. Antioxidant, ethylene and membrane leakage responses to powdery mildew infection of near-isogenic barley lines with various types of resistance. *Eur. J. Plant Pathol.* **2008**, *121*, 21–33. [CrossRef]

72. Jambagi, S.; Dunwell, J.M. Global transcriptome analysis and identification of differentially expressed genes after infection of Fragaria vesca with powdery mildew (*Podosphaera aphanis*). *Transcr. Open Access* **2015**, *3*, 1000106. [CrossRef]

73. Weng, K.; Li, Z.-Q.; Liu, R.-Q.; Wang, L.; Wang, Y.-J.; Xu, Y. Transcriptome of Erysiphe necator-infected Vitis pseudoreticulata leaves provides insight into grapevine resistance to powdery mildew. *Hortic. Res.* **2014**, *1*, 1–12. [CrossRef]

74. Molitor, A.; Zajic, D.; Voll, L.M.; Pons-Kühnemann, J.; Samans, B.; Kogel, K.-H.; Waller, F. Barley leaf transcriptome and metabolite analysis reveals new aspects of compatibility and Piriformospora indica–mediated systemic induced resistance to powdery mildew. *Mol. Plant Microbe Interact.* **2011**, *24*, 1427–1439. [CrossRef]

75. Seeholzer, S.; Tsuchimatsu, T.; Jordan, T.; Bieri, S.; Pajonk, S.; Yang, W.; Jahoor, A.; Shimizu, K.K.; Keller, B.; Schulze-Lefert, P. Diversity at the Mla powdery mildew resistance locus from cultivated barley reveals sites of positive selection. *Mol. Plant Microbe Interact.* **2010**, *23*, 497–509. [CrossRef]

76. Consonni, C.; Humphry, M.E.; Hartmann, H.A.; Livaja, M.; Durner, J.; Westphal, L.; Vogel, J.; Lipka, V.; Kemmerling, B.; Schulze-Lefert, P. Conserved requirement for a plant host cell protein in powdery mildew pathogenesis. *Nat. Genet.* **2006**, *38*, 716–720. [CrossRef] [PubMed]

77. Sanderfoot, A.A.; Assaad, F.F.; Raikhel, N.V. The Arabidopsis genome. An abundance of soluble N-ethylmaleimide-sensitive factor adaptor protein receptors. *Plant Physiol.* **2000**, *124*, 1558–1569. [CrossRef] [PubMed]

78. Bracuto, V.; Appiano, M.; Zheng, Z.; Wolters, A.-M.A.; Yan, Z.; Ricciardi, L.; Visser, R.G.; Pavan, S.; Bai, Y. Functional characterization of a syntaxin involved in tomato (*Solanum lycopersicum*) resistance against powdery mildew. *Front. Plant Sci.* **2017**, *8*, 1573. [CrossRef] [PubMed]

79. Pavan, S.; Jacobsen, E.; Visser, R.G.; Bai, Y. Loss of susceptibility as a novel breeding strategy for durable and broad-spectrum resistance. *Mol. Breed.* **2010**, *25*, 1. [CrossRef] [PubMed]

80. Reiner, T.; Hoefle, C.; Hückelhoven, R. A barley SKP1-like protein controls abundance of the susceptibility factor RACB and influences the interaction of barley with the barley powdery mildew fungus. *Mol. Plant Pathol.* **2016**, *17*, 184–195. [CrossRef]

81. Li, Y.; Qiu, L.; Liu, X.; Zhang, Q.; Zhuansun, X.; Fahima, T.; Krugman, T.; Sun, Q.; Xie, C. Glycerol-induced powdery mildew resistance in wheat by regulating plant fatty acid metabolism, plant hormones cross-talk, and pathogenesis-related genes. *Int. J. Mol. Sci.* **2020**, *21*, 673. [CrossRef]

82. Yang, G.; Liang, K.; Zhou, Z.; Wang, X.; Huang, G. UPLC-ESI-MS/MS-Based Widely Targeted Metabolomics Analysis of Wood Metabolites in Teak (*Tectona grandis*). *Molecules* **2020**, *25*, 2189. [CrossRef]

83. Chen, L.; Wu, Q.; He, W.; He, T.; Wu, Q.; Miao, Y. Combined De Novo Transcriptome and Metabolome Analysis of Common Bean Response to Fusarium oxysporum f. sp. phaseoli Infection. *Int. J. Mol. Sci.* **2019**, *20*, 6278. [CrossRef]

84. Grabherr, M.G.; Haas, B.J.; Yassour, M.; Levin, J.Z.; Thompson, D.A.; Amit, I.; Adiconis, X.; Fan, L.; Raychowdhury, R.; Zeng, Q.; et al. Full-length transcriptome assembly from RNA-Seq data without a reference genome. *Nat Biotech* **2011**, *29*, 644. [CrossRef]

85. Zeng, X.; Long, H.; Wang, Z.; Zhao, S.; Tang, Y.; Huang, Z.; Wang, Y.; Xu, Q.; Mao, L.; Deng, G.; et al. The draft genome of Tibian hulless barley reveals adaptive patterns to the high stressful Tibean Plateau. *PNAS* **2015**, *112*, 1095–1100. [CrossRef]

86. Kim, D.; Paggi, J.M.; Park, C.; Bennett, C.; Salzberg, S.L. Graph-based genome alignment and genotyping with HISAT2 and HISAT-genotype. *Nat. Biotechnol.* **2019**, *37*, 907–915. [CrossRef]

87. Trapnell, C.; Roberts, A.; Goff, L.; Pertea, G.; Kim, D.; Kelley, D.R.; Pimentel, H.; Salzberg, S.L.; Rinn, J.L.; Pachter, L. Differential gene and transcript expression analysis of RNA-seq experiments with TopHat and Cufflinks. *Nat. Protoc.* **2012**, *7*, 562–578. [CrossRef] [PubMed]

88. Varet, H.; Brillet-Guéguen, L.; Coppée, J.-Y.; Dillies, M.-A. SARTools: A DESeq2-and edgeR-based R pipeline for comprehensive differential analysis of RNA-Seq data. *PLoS ONE* **2016**, *11*, e0157022.

89. Liao, Y.; Smyth, G.K.; Shi, W. featureCounts: An efficient general purpose program for assigning sequence reads to genomic features. *Bioinformatics* **2014**, *30*, 923–930. [CrossRef] [PubMed]

90. Anders, S.; McCarthy, D.J.; Chen, Y.; Okoniewski, M.; Smyth, G.K.; Huber, W.; Robinson, M.D. Count-based differential expression analysis of RNA sequencing data using R and Bioconductor. *Nat Protoc.* **2013**, *8*, 1765. [CrossRef]

91. Heberle, H.; Meirelles, G.V.; da Silva, F.R.; Telles, G.P.; Minghim, R. InteractiVenn: A web-based tool for the analysis of sets through Venn diagrams. *BMC Bioinform.* **2015**, *16*, 1–7. [CrossRef] [PubMed]

92. Kanehisa, M.; Goto, S.; Kawashima, S.; Okuno, Y.; Hattori, M. The KEGG resource for deciphering the genome. *Nucleic Acids Res.* **2004**, *32*, D277–D280. [CrossRef]

93. Ashburner, M.; Ball, C.A.; Blake, J.A.; Botstein, D.; Butler, H.; Cherry, J.M.; Davis, A.P.; Dolinski, K.; Dwight, S.S.; Eppig, J.T.; et al. Gene Ontology: Tool for the unification of biology. *Nat. Genet.* **2000**, *25*, 25. [CrossRef]

94. Tatusov, R.L.; Galperin, M.Y.; Natale, D.A.; Koonin, E.V. The COG Database: A tool for fenome-scale analysis of protein functions and evolution. *Nucleic Acids Res.* **2000**, *28*, 33–36. [CrossRef]

95. Apweiler, R.; Bairoch, A.; Wu, C.H.; Barker, W.C.; Boeckmann, B.; Ferro, S.; Gasteiger, E.; Huang, H.; Lopez, R.; Magrane, M. UniProt: The universal protein knowledgebase. *Nucleic Acids Res.* **2004**, *32*, D115–D119. [CrossRef]

96. Koonin, E.V.; Fedorova, N.D.; Jackson, J.D.; Jacobs, A.R.; Krylov, D.M.; Makarova, K.S.; Mazumder, R.; Mekhedov, S.L.; Nikolskaya, A.N.; Rao, B.S. A comprehensive evolutionary classification of proteins encoded in complete eukaryotic genomes. *Genome. Biol.* **2004**, *5*, R7. [CrossRef] [PubMed]

97. Langmead, B.; Trapnell, C.; Pop, M.; Salzberg, S.L. Ultrafast and memory-efficient alignment of short DNA sequences to the human genome. *Genom. Biol.* **2009**, *10*, R25. [CrossRef]

98. Xie, C.; Mao, X.; Huang, J.; Ding, Y.; Wu, J.; Dong, S.; Kong, L.; Gao, G.; Li, C.-Y.; Wei, L. KOBAS 2.0: A web server for annotation and identification of enriched pathways and diseases. *Nucleic Acids Res.* **2011**, *39*, W316–W322. [CrossRef] [PubMed]

99. Chen, C.; Chen, H.; He, Y.; Xia, R. TBtools, a toolkit for biologists integrating various biological data handling tools with a user-friendly interface. *BioRxiv* **2018**, 289660. [CrossRef]

100. Walling, J.G.; Zalapa, L.A.; Vinje, M.A. Evaluation and selection of internal reference genes from two-and six-row US malting barley varieties throughout micromalting for use in RT-qPCR. *PLoS ONE* **2018**, *13*, e0196966. [CrossRef]